90-14

A scaling-dimensionality transform and the level-crossing activity of stationary normal processes.

André Barbé

ESAT-SISTA report 1990-14
Department of Electrical Engineering
Katholieke Universiteit Leuven
Kardinaal Mercierlaan 94
B-3030 Heverlee
Belgium
tel: 32/16/220931
fax: 32/16/221855
email: barbe@esat.kuleuven.ac.be

June 14, 1990

Other ESAT-SISTA Reports

The following **ESAT-SISTA** reports can also be obtained. Contact the authors or write to *Ingrid Tokka*, ESAT-SISTA, Katholieke Universiteit Leuven, Kardinaal Mercierlaan 94, B-3030 Leuven (Heverlee), Belgium.
tel:32/16/220931, fax:32/16/221855, email: tokka@esat.kuleuven.ac.be
A complete list of more than 200 publications is also available.

- S. Van Huffel, Vandewalle J. *Analysis and properties of the generalized total least squares problem $AX \approx B$ when some or all columns of A are subject to errors.* ESAT-SISTA Report 1989-17, 21 pp., July 1989, Department of Electrical Engineering, Katholieke Universiteit Leuven, Belgium. (Appeared in SIAM J. on Matrix Analysis and Applic., 10, no.3, pp.294-315, July 1989).
- Tan S., Vandewalle J. *An alternative proof for the minimal factorization theorem for rational matrices.* ESAT-SISTA report 1989-18, 6 pp., July 1989, Department of Electrical Engineering, Katholieke Universiteit Leuven, Belgium.
- Tan S., Vandewalle J. *On prime factors of nonsingular rational matrices.* ESAT-SISTA report 1989-19, 10 pp., September 1989, Department of Electrical Engineering, Katholieke Universiteit Leuven, Belgium.
- Tan S., Vandewalle J. *Comments on 'A neural net approach to discrete Hartley and Fourier Transforms'.* ESAT-SISTA report 1989-20, 4 pp., September 1989, Department of Electrical Engineering, Katholieke Universiteit Leuven, Belgium.
- De Moor B., Zha H. *A tree of generalizations of the ordinary singular value decomposition.* ESAT-SISTA Report 1989-21, 35 pp., October 1989, Department of Electrical Engineering, Katholieke Universiteit Leuven, Belgium.
- Zha H. *Analysis and Numerical Solution of Fixed Rank Matrix Approximation with General Weighting Matrices.* ESAT-SISTA Report 1989-22, 28 pp., October 1989, Department of Electrical Engineering, Katholieke Universiteit Leuven, Belgium.
- Moonen M., Van Dooren P., Vandewalle J. *Parallel Updating Algorithms, Part II: Generalized Singular Value Decompositions.* ESAT-SISTA Report 1989-23, 29 pp., October 1989, Department of Electrical Engineering, Katholieke Universiteit Leuven, Belgium.
- Zha H. *On the quotient singular value decomposition.* ESAT-SISTA Report 1989-24, 14 pp., November 1989, Department of Electrical Engineering, Katholieke Universiteit Leuven, Belgium.
- Zha H. *The implicit QR Decomposition and its applications.* ESAT-SISTA report 1989-25, 19 pp., November 1989, Department of Electrical Engineering, Katholieke Universiteit Leuven, Belgium.
- Moonen M., Vandewalle J. *RLS with stabilized inverse factorization.* ESAT-SISTA report 1989-26, 16 pp., December 1989, Department of Electrical Engineering, Katholieke Universiteit Leuven, Belgium.
- Moonen M., Vandewalle J. *A systolic array for square root Kalman filtering.* ESAT-SISTA report 1989-27, 14 pp., December 1989, Department of Electrical Engineering, Katholieke Universiteit Leuven, Belgium.
- De Moor B., Boyd S. *Analytic properties of singular values and vectors.* ESAT-SISTA Report 1989-28, 17 pp., December 1989, Department of Electrical Engineering, Katholieke Universiteit Leuven, Belgium.
- Suykens J., Moonen M., Vandewalle J. *A survey of SVD-applications, specifications and systolic architectures.* ESAT-SISTA Report 1989-29, 10 pp., November 1989, Department of Electrical Engineering, Katholieke Universiteit Leuven, Belgium.

- Vandenberghe L., Vandewalle J., *Variable dimension algorithms for solving resistive circuits.*, ESAT-SISTA Report 1990-01, 50 pp., February 1990, Department of Electrical Engineering, Katholieke Universiteit Leuven, Belgium.
- Bart De Moor. *Total linear least squares with inequality constraints*, ESAT-SISTA Report 1990-02, Department of Electrical Engineering, Katholieke Universiteit Leuven, Belgium, 25 pp., March 1990.
- Sabine Van Huffel, *Iterative algorithms for computing the singular subspace of a matrix associated with its smallest singular values*, ESAT-SISTA Report 1990-03, Department of Electrical Engineering, Katholieke Universiteit Leuven, Belgium, 31 pp., March 1990.
- Sabine Van Huffel, *Chebyshev Acceleration Techniques for solving slowly varying total least squares problems*, ESAT-SISTA Report 1990-04, Department of Electrical Engineering, Katholieke Universiteit Leuven, Belgium, 20 pp., April 1990.
- De Moor B., Gevers M., Goodwin G. *Estimation of transfer functions: overbiased, underbiased and unbiased identification schemes.* ESAT-SISTA Report 1990-05, Department of Electrical Engineering, Katholieke Universiteit Leuven, Belgium, 33 pp., May 1990.
- De Moor B., Vandenberghe L., Vandewalle J. *The generalized linear complementarity problem and an algorithm to find all its solutions.* ESAT-SISTA Report 1990-06, Department of Electrical Engineering, Katholieke Universiteit Leuven, Belgium, 30 pp., May 1990. (Reworked and extended version of ESAT-SISTA Report 1989-04, submitted for publication.)
- Callaerts D., Vandewalle J., Van Compernolle D., *OSVD and QSVD in Signal Separation*, ESAT-SISTA Report 1990-07, Department of Electrical Engineering, Katholieke Universiteit Leuven, Belgium, 8 pp., May 1990.
- Tan S., *Hopfield Hetero-associative Nets, Bipartite Operation and BAM*, ESAT-SISTA Report 1990-08, Department of Electrical Engineering, Katholieke Universiteit Leuven, Belgium, 8 pp., May 1990.
- Tan S., Vandenberghe L., Vandewalle J., *Remarks on the stability of asymmetric dynamical neural networks*, ESAT-SISTA Report 1990-09, Department of Electrical Engineering, Katholieke Universiteit Leuven, Belgium, 7 pp., May 1990.
- Tan S., Vandewalle J., *Principles of dynamical neural network structure and adaptive learning*, ESAT-SISTA Report 1990-10, Department of Electrical Engineering, Katholieke Universiteit Leuven, Belgium, 20 pp., May 1990.
- De Moor B., Zha H.,*A tree of generalizations of the ordinary singular value decomposition.*, ESAT-SISTA Report 1990-11, Department of Electrical Engineering, Katholieke Universiteit Leuven, Belgium, 24 pp., June 1990 (Accepted for the special issue on 'Matrix Canonical Forms' of 'Linear Algebra and its Applications').
- De Moor B., *On the structure of generalized singular value decompositions.*, ESAT-SISTA Report 1990-12, Department of Electrical Engineering, Katholieke Universiteit Leuven, Belgium, June 1990.
- De Moor B., *Generalizations of the OSVD, Structure, Properties and Applications*, ESAT-SISTA Report 1990-13, Department of Electrical Engineering, Katholieke Universiteit Leuven, Belgium, June 1990.
- Barbé A., *A scaling-dimensionality transform and the level-crossing activity of stationary normal processes.*, ESAT-SISTA Report 1990-14, Department of Electrical Engineering, Katholieke Universiteit Leuven, Belgium, June 1990.

A SCALING-DIMENSIONALITY TRANSFORM AND THE LEVEL-CROSSING ACTIVITY OF STATIONARY NORMAL PROCESSES

A. Barbé
Department of Electrical Engineering
Katholieke Universiteit Leuven
Kardinaal Mercierlaan 94
B-3030 HEVERLEE - BELGIUM
e-mail : barbe@esat.kuleuven.ac.be

Abstract

The scaling-dimensionality transform $D_a(r,\theta)$ of stochastic processes is introduced as a generalization of the fractal dimension concept over an infinite range of time scales. It is based on the expected number of crossings of a constant level a, and is a function of two variables : the scaling factor r and the sampling time θ. General properties of this transform are discussed, whereby $D_a(1,\theta)$ emerges as the crucial transform. Results for stationary Gaussian processes, calculable from Rice's formula, are presented. $D_a(r,\theta)$ is always finite, even for $\theta \to 0$, as opposed to the level-crossing rate which is infinite for many signal models. For $\theta \to 0$, $D_a(r,\theta)$ corresponds to the fractal dimension of a related fractional Brownian motion as considered by B. Mandelbrot. The concept of controllable signal-blurring is introduced, and its influence on the $D_a(r,\theta)$-transform is analyzed. This allows for a well-argued assessment of the level-crossing activity of these signals, resulting in a balanced choice of both amplitude- and time-scale for discretized signal representations.

1 Introduction : level-crossings, fractal noises, fractal dimensions.

Level-crossing problems of stochastic processes have received a widely spread interest during the last four decades. They have been dealt with in theoretical contributions and in several signal processing applications, and seem to be among the tougher problems for

[1] Part of this paper was presented at the IEEE International Symposium on Information Theory, San Diego, January 1990.

which only partial solutions under specific conditions are known or practicable. For an overview, see the 1973 paper by I. Blake and W. Lindsey [1] and the 1986 update of J. Abrahams [2].
The problem this paper is facing, is the one of finding a practically useful measure for the mean level-crossing activity of stationary normal processes. As witnessed by A.J. Rainal [3], early contributions about the average rate of level-crossings were made by S.O. Rice in 1936 and resulted in a famous formula [4] bearing this scientist's name (although also M. Kac [5] seems to have obtained similar results independently). This formula will play a basic role in a large part of this paper. For a stationary process $x(t)$, the formula gives the expected number of crossings of a constant level a :

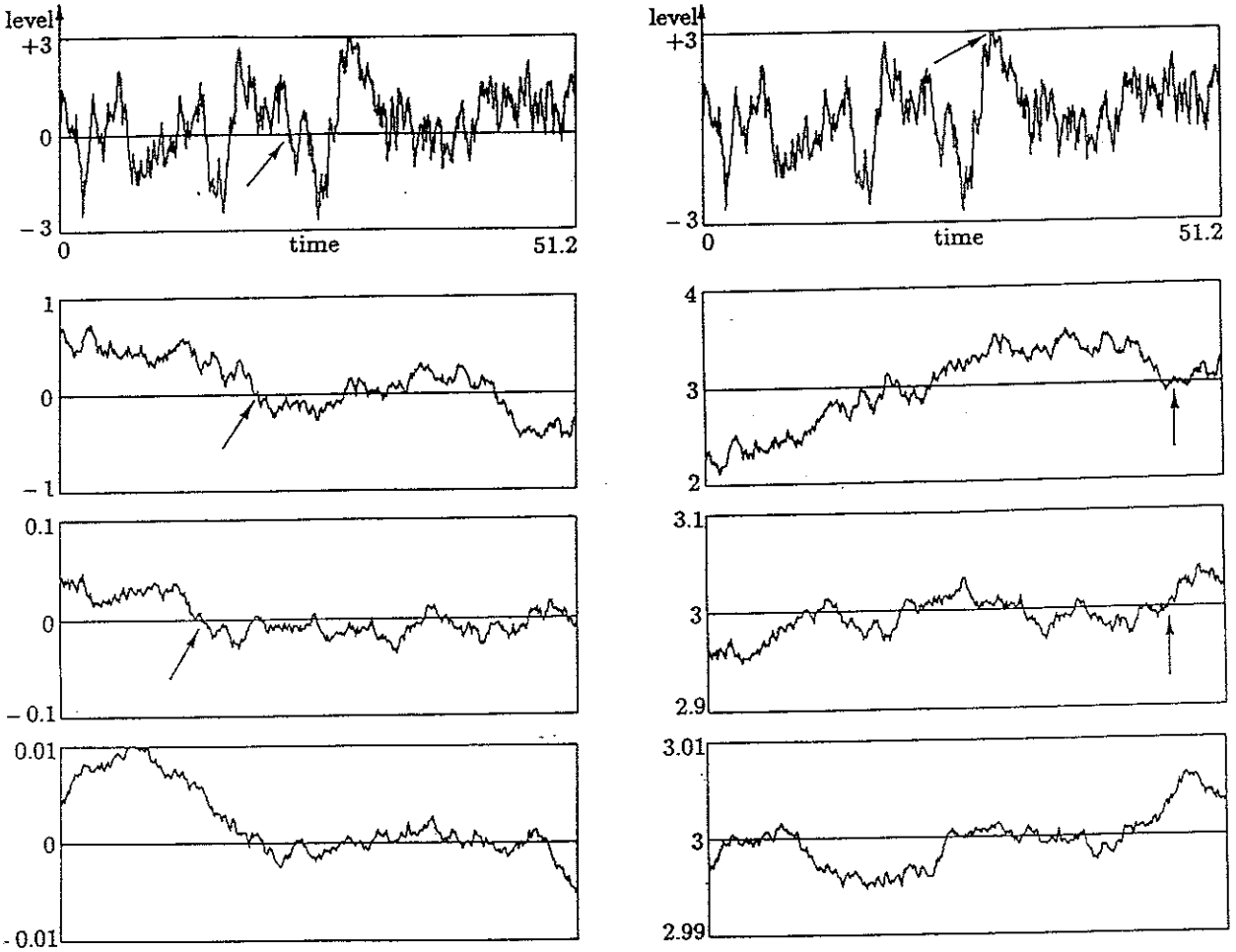
$$EN_a(T_0) = T_0 \int_{-\infty}^{+\infty} |\dot{x}| f_{x\dot{x}}(a, \dot{x}) d\dot{x} \quad . \tag{1}$$

$N_a(T_0)$ represents the number of crossings (upward and downward) of the level a over an observation interval of duration T_0. $f_{x\dot{x}}(\cdot,\cdot)$ is the joint probability density of $x(t)$ and its derivative $\dot{x}(t)$. In case the process is also *Gaussian* with autocovariance function $R(\tau)$, formula (1) transforms into

$$EN_a(T_0) = -\frac{T_0}{\pi} \left[\frac{-\ddot{R}(0)}{R(0)}\right]^{\frac{1}{2}} exp(-a^2/2R(0)) \, . \tag{2}$$

However, since a lot of signals are modelled by covariance functions which are non-differentiable at the origin, meaning that the signals themselves are not differentiable in the mean square sense (see e.g. [6]), this formula gives problems. A formal application of (2) in these cases results in $EN_a(T_o) = \infty$. Although this is a mathematically correct and senseful result, it is practically useless. The reason is that (2) counts every crossing of the level considered, even those on the very ultimate microscopic scales. As the common nondifferentiable processes have a power spectrum that behaves as $1/f^2$ for large frequencies, they resemble the $1/f^2$ noise on a microscopic time scale. This $1/f^2$ noise is the well-known Brownian motion or Wiener-Lévy process, and belongs to the category of Gaussian processes with spectrum $1/f^\beta (1 < \beta < 3)$. These have been called *fractional Brownian motions* by Mandelbrot and Van Ness [7]. Since Mandelbrot [8] introduced the concept of *fractals*, it is known that these Brownian noises are fractal or *scaling* noises. These are *self-affine* on all scales (see Voss [9]), and therefore they exhibit level-crossings on all scales. Figure 1 shows this for a signal with autocovariance $R(\tau) = exp(-|\tau|)$.

Practical signal representations are never available at the infinitely high resolutions in time and amplitude necessary to show these microscopic details, and there is no need for this indeed. Applications only require sufficient detail up to a certain scale. For each selected time resolution (the sampling distance θ), there is a corresponding acceptable amplitude resolution, so that redundancy as well as lack of desirable detail in the representation are avoided. This is also related to the problem of finding the proper time and amplitude resolution for assessing the mean macroscopic level-crossing activity of a signal.
An attempt to obtain such practicable level-crossing measure was presented earlier by the



a. b.

Figure 1: Zooming in on microscopic details around a level crossing for a sample of the Gaussian process with autocovariance $R(\tau) = \exp(-|\tau|)$: (a) for level 0, (b) for level 3. Each of the pictures represents a 128 x enlargement in time scale of the picture just above in the vicinity indicated by the arrow. Notice the different scaling in amplitude, and the statistical similarity of all six lower images.

author [10]. It was based on the determination of the mean number of level crossings for an equidistantly sampled and linearly interpolated version of the signals considered, whereby the sampling period was determined in a plausible *standardized* way. In what follows, this problem will be revisited and the selection of the sampling interval will be based on more fundamental concepts that remind of fractal dimensional analysis.

Indeed, the above mentioned fractional noises can be characterized by a fractal dimension ([8],[9],[7]). The so-called *scaling dimension* D (or *similarity-*, or *fractal* dimension) of a fractal set F will be reconsidered briefly. Following Barnsley [11], it may be defined by

$$D \triangleq \lim_{\epsilon \to o} \frac{\log N(\epsilon)}{\log 1/\epsilon} \quad , \tag{3}$$

where $N(\epsilon)$ is the minimal number of closed balls of radius ϵ that are needed to cover the set F. D has typically a non-integer value for fractal sets, although this is not a necessity. For the $1/f^{\beta}$-Brownian motions, it is known [9] that

$$D = \frac{5-\beta}{2} \quad . \tag{4}$$

D is also related to the *statistical self-affine* property of the signal, stating that $X(rt)$ is *statistically* equivalent to the process $r^H X(t)$, where

$$H = 2 - D = \frac{\beta - 1}{2} \quad . \tag{5}$$

The set of points obtained by intersecting the fractal curve representing a realization of the stochastic $1/f^{\beta}$-signals with a horizontal line, has been called the *zero-set* of the process. It is a *statistically self-similar* point set with fractal dimension $D_0 = D - 1$. [Voss [9]p.45, Mandelbrot [8]p. 237].
Scaling the dimension of the elementary box of size ϵ by a factor r changes (3) into

$$D = \lim_{\epsilon \to 0} \frac{\log N(r\epsilon)}{\log 1/r\epsilon} \quad . \tag{6}$$

The combination of (3) and (6) produces an alternative definition for D :

$$r^D = \lim_{\epsilon \to 0} \frac{N(\epsilon)}{N(r\epsilon)} \tag{7}$$

or, equivalently :

$$D = \lim_{\epsilon \to 0} \frac{\log N(\epsilon) - \log N(r\epsilon)}{\log r} \quad . \tag{8}$$

Notice that these definitions for D are related to the limiting case $\epsilon \to 0$. But for many classical examples of fractals in the literature, they hold for many ϵ and r, without the need for ϵ to go to zero. A typical example is given by the triadic Cantor set on [0,1] (see e.g. [8],[11]), where it is found that for any integers $k, j (k \geq 0, k + j \geq 0)$:

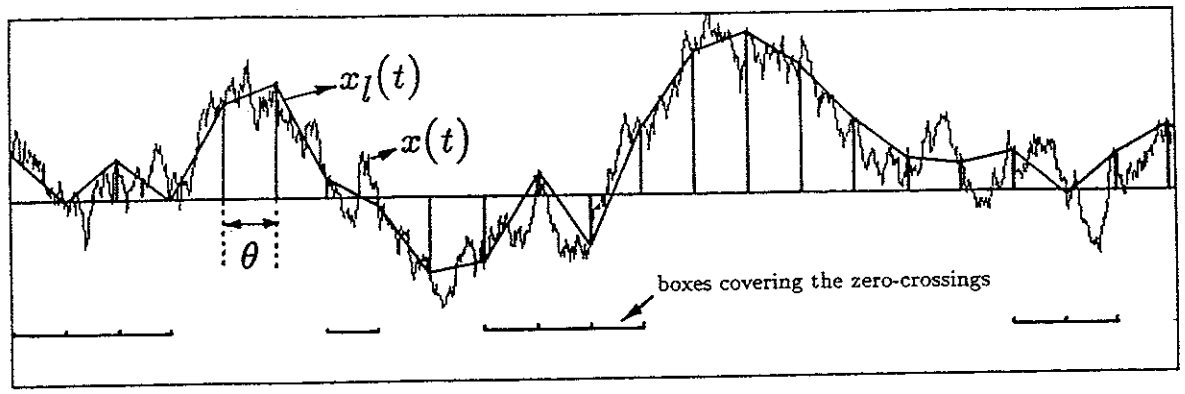


Figure 2: A realization of the process $x(t)$ and of one of its sampled and linearly interpolated versions $x_l(t;\theta)$.

$$\frac{N(3^{-k})}{N(3^{-j}3^{-k})} = (3^{-j})^{D(k,j)}, \text{ with } D(k,j) = \frac{\log 2}{\log 3} = \text{ constant} \tag{9}$$

In what follows, level-crossings will be at the heart of our interest. These level-crossings will be considered as point sets for which relevant information can be found in the *scaling dimension* $D(r,\varepsilon)$ defined as

$$r^{D(r,\varepsilon)} \triangleq N(\varepsilon)/N(r\varepsilon) \tag{10}$$

in analogy with expression (7). But here D is no longer independent of ε, nor of the scaling factor r. Also, the limiting condition $\varepsilon \to 0$ will be dropped. Instead, the limit $r \to 1$ will play an important role. Section 2 will deal with general properties of $D(r,\varepsilon)$, while sections 3 and 4 will concentrate on the Gaussian case.

2 The scaling-dimensionality transform for stationary stochastic processes.

2.1 Definition

Consider a stationary process $x(t)$. The process $x_l(t;\theta)$ is the linearly interpolated version of $x(t)$ when sampled with period θ, while the sampling origin is uniformly distributed in $[0,\theta]$ in order to stationarize the process (figure 2). Denote by $EN_a(T_0,\theta)$ the expected number of crossings of the level a by $x_l(t;\theta)$ over an observation interval T_0. With $EN_a(\theta)$ representing the mean number of level crossings per time unit ($\triangleq EN_a(1,\theta)$), the stationarity of the signal implies

$$EN_a(T_0,\theta) = T_0 EN_a(\theta) \ . \tag{11}$$

Referring to the so-called box counting techniques [11], this also represents the expected number of boxes (here : line segments) of size θ that cover the crossings of the level a,

under the restriction that the boxes are placed between the sampling instants.

Now define the *scaling-dimensionality transform* $D_a(r,\theta)$ of the set of crossings of the constant level a, in analogy with what was presented in the introduction, by the equation

$$r^{D_a(r,\theta)} \triangleq \frac{EN_a(T_0,\theta)}{EN_a(T_0,r\theta)} \overset{(11)}{=} \frac{EN_a(\theta)}{EN_a(r\theta)} \ . \tag{12}$$

$D_a(r,\theta)$ is normally defined for all positive $r \neq 1$ and for all $\theta > 0$. Equation (12) can be made explicit in $D_a(r,\theta)$:

$$D_a(r,\theta) \triangleq \frac{\log EN_a(\theta) - \log EN_a(r\theta)}{\log r} \ . \tag{13}$$

$D_a(r,\theta)$ is a function of the two variables (r,θ). Of central importance, at least for analytical purposes will be the particular function $D_a(1,\theta)$, defined by

$$D_a(1,\theta) \triangleq \lim_{r\to 1} D_a(r,\theta) \tag{14}$$

provided that this limit exists.

Figure 3 shows $D_0(r,\theta)$ for some Gaussian signals with interesting covariance function. The exact analytical expressions will be derived in later sections. $D_a(r,\theta)$ will normally be plotted on a linear scale with θ as variable on a log-scale, and with r and/or a as parameter. Notice that continuity, differentiability and analyticity of $D_a(r,\theta)$ with respect to (a,r,θ) depend on the very same properties of $EN_a(\theta)$ and $EN_a(r\theta)$ in a straightforward way. The limit $D_a(1,\theta)$ in (14) exists when $EN_a(\theta)$ is continuous in θ.

2.2 Properties of $D_a(r,\theta)$.

Property 2.1 : *Equivalence property for inverse scaling factors.*

$$D_a(r,\theta) = D_a(r^{-1},r\theta) \ . \tag{15}$$

This property follows directly from the definition (12). With logarithmic θ - scale, $D_a(r^{-1},r\theta)$ is congruent with $D_a(r,\theta)$ but horizontally shifted over a distance $-\log r$ (see e.g. fig. 3).

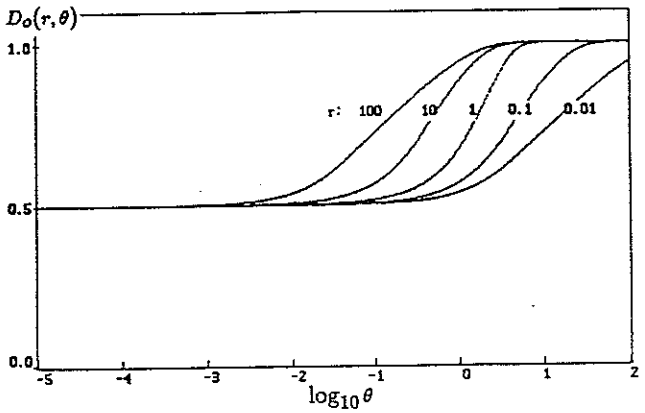
Property 2.2 :*Consistency equation in discrete form.*

Consider a discrete factorization of the scaling factor :

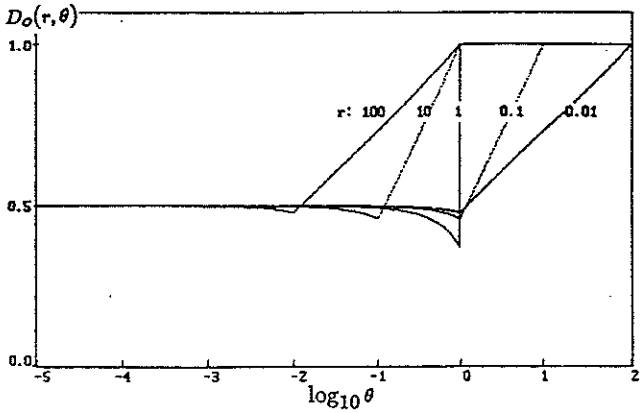
$$r = \prod_{k=1}^{N} r_k \qquad (\text{all } r_k > 0), \tag{16}$$

then it holds that

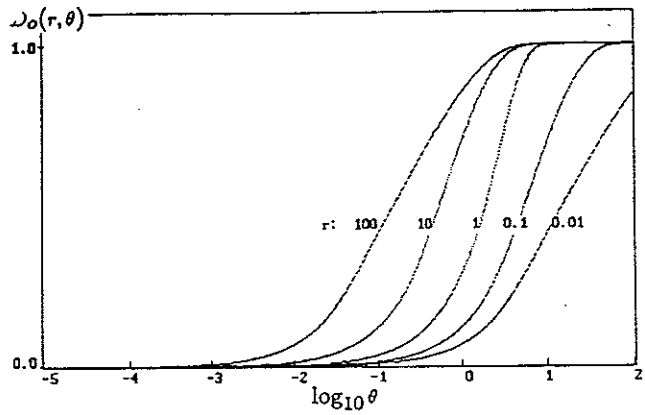
$$r^{D_a(r,\theta)} = r_1^{D_a(r_1,\theta)} r_2^{D_a(r_2,r_1\theta)} r_3^{D_a(r_3,r_2r_1\theta)} \ldots r_N^{D_a(r_N,r_{N-1}\ldots r_2r_1\theta)} \ . \tag{17}$$

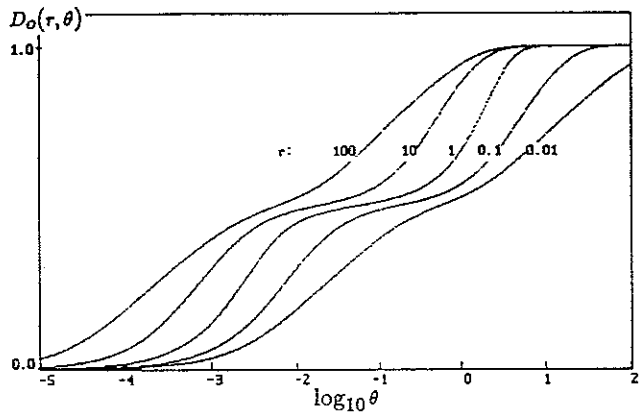


a. $R(\tau) = \exp(-|\tau|)$

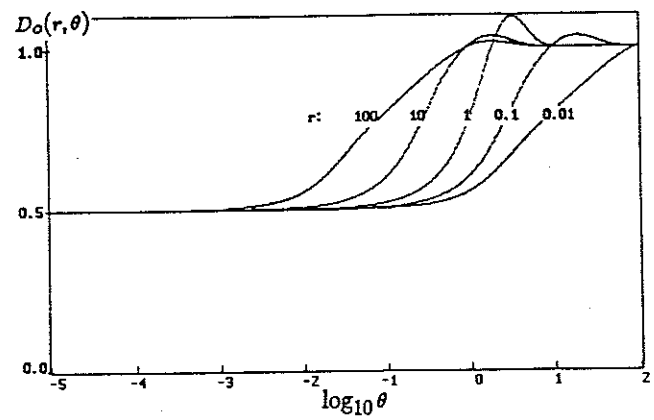


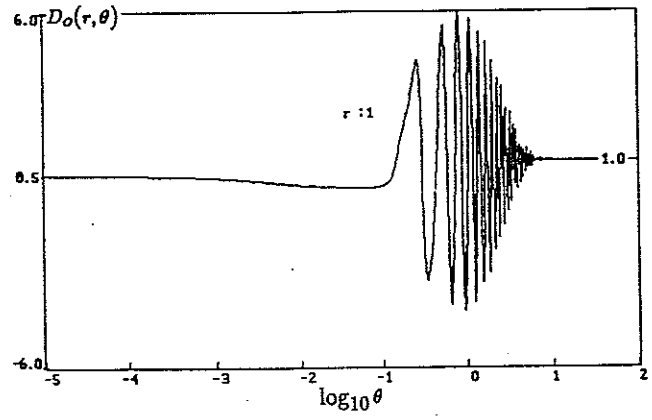
b. $R(\tau) = \max(0, 1 - |\tau|)$





c. $R(\tau) = \frac{1}{1-\beta}[\exp(-|\tau|) - \beta\exp(-|\tau|/\beta)]$, $\beta = 0.9$ d. $R(\tau)$ as in c., with $\beta = 0.01$





e. $R(\tau) = \frac{1}{\beta-1}[\beta\exp(-|\tau|) - \exp(-|\tau|/\beta)]$, $\beta = 0.9$ f. $R(\tau) = \exp(-|\tau|)\cos\frac{2\pi\tau}{\beta}$, $\beta = 0.3$

Figure 3: $D_0(r,\theta)$ for Gaussian signals with different covariance functions $R(\tau)$.

Proof : Observe that, with $r_0 \triangleq 1$, and using the definition (12) :

$$r^{D_a(r,\theta)} \overset{(12)}{=} \frac{EN_a(\theta)}{EN_a(r\theta)} = \prod_{k=1}^{N} \frac{EN_a((\prod_0^{k-1} r_j)\theta)}{EN_a(r_k(\prod_0^{k-1} r_j)\theta)} \overset{(12)}{=} \prod_{k=1}^{N} r_k^{D_a(r_k,(\prod_0^{k-1} r_j)\theta)} \tag{18}$$

Corollary :
An equivalent expression for (17) is obtained by taking the logarithms of both sides :

$$D_a(r,\theta)\log r = \sum_{k=1}^{N} D_a(r_k,(\prod_{j=0}^{k-1} r_j)\theta)\log r_k \tag{19}$$

or :

$$D_a(r,\theta) = \sum_{k=1}^{N} w_k D_a(r_k,(\prod_{j=0}^{k-1} r_j)\theta) \tag{20}$$

with

$$w_k = \log r_k / \log r = \log_r r_k \quad . \tag{21}$$

This means that $D_a(r,\theta)$ can be found as logarithmically averaged values of $D_a(r_k,\theta_k)$ at scaling values r_k whose product equals r and at properly modified sampling distances

$$\theta_k = (\prod_{j=0}^{k-1} r_j)\theta \quad .$$

Taking $r = r_1 r_2 = 1$ in (18) results in property 2.1.

Property 2.3 :*Consistency equation in continuous form.*

$$\text{For } r \neq 1 : D_a(r,\theta) = \frac{1}{\log r}\int_{\log\theta}^{\log r\theta} D_a(1,\zeta)d\log\zeta \quad . \tag{22}$$

Proof:
Consider first the case $r < 1$. Take $r_k = r^{1/N}$, with N an arbitrary integer. Use (20) to obtain

$$D_a(r,\theta) = \frac{1}{N}\sum_{k=0}^{N-1} D_a(r^{1/N}, r^{k/N}\theta) \quad . \tag{23}$$

Introduce $\zeta(x) \triangleq r^x\theta$, then $d\zeta(x) = \theta r^x \log r dx = \zeta(x)\log r dx$. Then (23) can be written as

$$D_a(r,\theta) = \sum_{k=0}^{N-1} \frac{D_a(r^{1/N},\zeta(x))}{\zeta(x)\log r} \cdot \frac{d\zeta(x)}{dx}|_{x=\frac{k}{N}} \cdot \frac{1}{N} \tag{24}$$

In this summation however, x changes discretely with steps $\Delta x = 1/N$. Now let $N \to \infty$, then $r^{1/N} \to 1, \Delta x \to 0$ and $d\zeta(x)/dx$ can be replaced by $\Delta\zeta(x)/\Delta x$. In the limit, (24) tends to

$$\frac{1}{\log r}\int_{\theta}^{r\theta}\frac{D_a(1,\zeta)}{\zeta}d\zeta \quad . \tag{25}$$

This form is equivalent to (22). Using property 2.1 (eqn. 15) allows to show that (22) also holds for $r > 1$ when it holds for $r < 1$.

Remark : Equation (22) gives a special meaning to $D_a(1,\theta)$. It is *most fundamental* as the dimension for scaling factors $r \neq 1$ can be considered as logarithmic averages of $D_a(1,\theta)$. Using the most convenient way of plotting $D_a(r,\theta)$, where θ is set out logarithmically, equation (22) has a pretty direct interpretation as the ordinary average value of $D_a(1,\zeta)$ in the interval $\log(r\theta,\theta)$.
Thinking about possible measurements however, it is clear that $D_a(1,\theta)$ according to its definition (13,14) is not directly measurable. On the other hand, measurements of $D_a(r,\theta)$ for r different from 1 seem plausible. The next properties may be helpful in relating $D_a(1,\theta)$ to $D_a(r \neq 1,\theta)$.

Property 2.4 :*Differential form for* $D_a(r,\theta)$

Where $D_a(r,\theta)$ is differentiable in both variables r and θ, $D_a(r,\theta)$ satisfies the following set of equations which can be derived from differentiation of (22)

$$\frac{\partial D_a(r,\theta)}{\partial \log r} = \frac{D_a(1,r\theta) - D_a(r,\theta)}{\log r} \tag{26}$$

$$\frac{\partial D_a(r,\theta)}{\partial \log \theta} = \frac{D_a(1,r\theta) - D_a(1,\theta)}{\log r} \quad . \tag{27}$$

Eliminating $D_a(1,r\theta)$ in (26), (27) gives

$$\frac{\partial D_a(r,\theta)}{\partial \log r} - \frac{\partial D_a(r,\theta)}{\partial \log \theta} = \frac{D_a(1,\theta) - D_a(r,\theta)}{\log r} \quad . \tag{28}$$

Remark : Equation (28) allows $D_a(1,\theta)$ to be recovered from knowledge of $D_a(r_c,\theta)$ in a small neighborhood of r_c. When it should occur that left and right derivatives differ in some points, the equations above should be interpreted in the corresponding way.

Property 2.5 :

If $D_a(r,\theta)$ is differentiable at $(1,\theta)$, then

$$\frac{\partial D_a(1,\theta)}{\partial r} = \frac{1}{2}\frac{\partial D_a(1,\theta)}{\partial \log \theta} \quad \text{or,as} \quad r = 1 : \frac{\partial D_a(1,\theta)}{\partial \log r} = \frac{1}{2}\frac{\partial D_a(1,\theta)}{\partial \log \theta} \quad . \tag{29}$$

Proof : the differentiability implies that for r close to 1

$$D_a(r,\theta) = D_a(1,\theta) + \frac{\partial D_a(1,\theta)}{\partial r}(r-1) + o(r-1) \ , \tag{30}$$

and (28) becomes

$$r\frac{\partial D_a(r,\theta)}{\partial r} - \frac{\partial D_a(r,\theta)}{\partial \log\theta} = \frac{1-r}{\log r}\frac{\partial D_a(1,\theta)}{\partial r} + \frac{o(r-1)}{\log r} \ . \tag{31}$$

Let $r \to 1$ in this equation to obtain (29).

Corollary : Consider the contours of constant $D_a(r,\theta)$ in the $(\log\theta, r)$– or $(\log\theta, \log r)$-plane. The tangent at these contours along $r = 1$ all have the same direction, independent of the particular value of the constant. This direction is given by $dr = -2d\log\theta$ (or $d\log r = -2d\log\theta$) (figure 4). So in the neighbourhood of $r = 1, D_a(r,\theta)$ is a quasi-undistorted shifted version of $D_a(1,\theta)$ along that direction (as far as the first order approximation is concerned). Indeed, the condition for the differential $dD_a(1,\theta)$to be zero is

$$dD_a(1,\theta) = \frac{\partial D_a(1,\theta)}{\partial r}dr + \frac{\partial D_a(1,\theta)}{\partial \theta}d\theta = 0 \ .$$

With $\frac{\partial D_a(1,\theta)}{\partial \theta}d\theta = \frac{\partial D_a(1,\theta)}{\partial \log\theta}d\log\theta$, and using (29), this condition transforms into

$$dr/d\log\theta \mid_{r=1} = -2 \ \ (\text{or} \ \ d\log r/d\log\theta \mid_{r=1} = -2) \ . \tag{32}$$

A case for which the differentiability condition does not hold at $\theta = 1$ is the one represented in figure 3b.

Property 2.6 :
If $D_a(r,\theta)$ is differentiable at $(1,\theta)$, then it holds that for r *close to 1* :

$$D_a(1,\theta) \simeq D_a(r, r^{-\frac{1}{2}}\theta) \ . \tag{33}$$

Proof : According to property 2.1 (eqn. 15),

$$D_a(1+\Delta r, \theta_0) = D_a(\frac{1}{1+\Delta r}, (1+\Delta r)\theta_0) \ .$$

This means that the straight line connecting the points $(1+\Delta r, \theta_0)$ and $(\frac{1}{1+\Delta r}, (1+\Delta r)\theta_0)$ on the D_a surface is horizontal and has slope $d\log r/d\log\theta = -2$ in the $(\log r, \log\theta)$-plane (see figure 4). For sufficiently small Δr, this line nearly coincides with the tangent on the constant-D_a contour (cf. property 2.5). Through linear interpolation between $D_a(1+\Delta r, \theta_0)$ and $D_a(\frac{1}{1+\Delta r}, (1+\Delta r)\theta_0)$, one finds $D_a(1, (1+\Delta r)^{\frac{1}{2}}\theta_0) = D_a(1+\Delta r, \theta_0)$. Replacing $(1+\Delta r)^{\frac{1}{2}}\theta_0$ by θ and $1+\Delta r$ by r gives (33).

Property 2.7. :$D_a(1,\theta)$ *as the relative sensitivity of* $EN_a(\theta)$ *with respect to* θ.

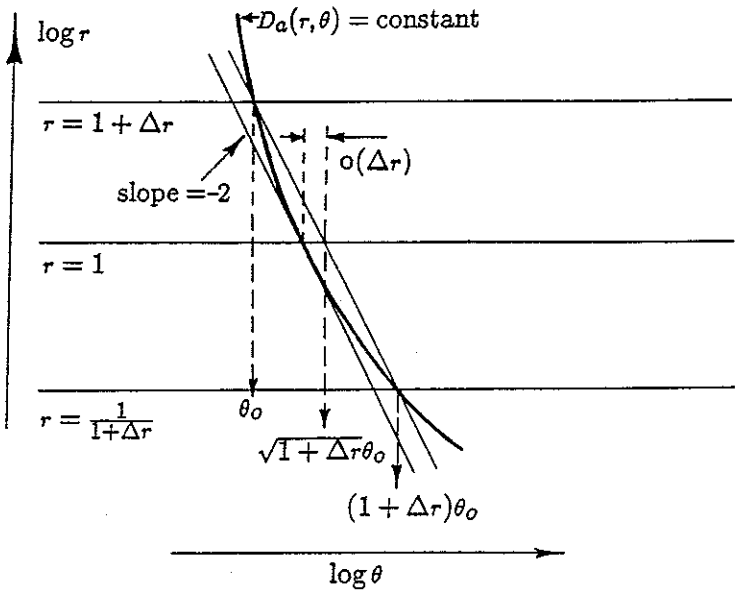


Figure 4: Behaviour of $D_a(r,\theta) =$ constant in the neighbourhood of $r = 1$.

If $EN_a(\theta)$ is differentiable in θ, then

$$D_a(1,\theta) = -\frac{\partial \log EN_a(\theta)}{\partial \log \theta} = -\frac{\theta}{EN_a(\theta)}\frac{\partial EN_a(\theta)}{\partial \theta} \quad . \tag{34}$$

Proof : Let $r = 1 + \Delta r$, then differentiability implies

$$\log EN_a((1+\Delta r)\theta) = \log EN_a(\theta) + \frac{\partial \log EN_a(\theta)}{\partial \theta}\Delta r \cdot \theta + o(\Delta r\theta) \quad .$$

Using this in the $D_a(r,\theta)$-definition (13), gives

$$D_a(1+\Delta r,\theta) = -\frac{\Delta r}{\log(1+\Delta r)}\frac{\partial \log EN_a(\theta)}{\partial \theta}\theta + \frac{o(\Delta r\theta)}{\log(1+\Delta r)} \quad .$$

Taking the limit of this expression for $\Delta r \to 0$ produces (34).

Property 2.8 : *Merging of two signals.*

Consider an observation interval T_0 split up in a number of subintervals. Some of these subintervals are filled with a signal of dimensionality $D_a^1(r,\theta)$, the remaining ones with a signal of dimensionality $D_a^2(r,\theta)$. The total length of these two types of subintervals will be represented by T_{01} and T_{02} (so $T_0 = T_{01} + T_{02}$). From the definition, we know that

$$r^{D_a^1(r,\theta)} = \frac{EN_a^1(T_{01},\theta)}{EN_a^1(T_{01},r\theta)}$$

and

$$r^{D_a^2(r,\theta)} = \frac{EN_a^2(T_{02},\theta)}{EN_a^2(T_{02},r\theta)} \quad .$$

The dimensionality $D_a^3(r,\theta)$ for the whole signal over T_0 thus obtained, is then found to be given by

$$\begin{aligned} r^{D_a^3(r,\theta)} &= \frac{E[N_a^1(T_{01},\theta) + N_a^2(T_{02},\theta)]}{E[N_a^1(T_{01},r\theta) + N_a^2(T_{02},r\theta)]} \\ &= r^{D_a^1(r,\theta)}[\frac{1+\lambda(\theta)}{1+r^{D_a^1(r,\theta)-D_a^2(r,\theta)}\cdot\lambda(\theta)}] \\ &= r^{D_a^1(r,\theta)}r^{\Delta[r,\lambda(\theta)]} \quad , \end{aligned} \tag{35}$$

with $\lambda(\theta) \triangleq EN_a^2(T_{02},\theta)/EN_a^1(T_{01},(\theta)$ the ratio of the expected total number of level crossings in both interval-types at sampling period θ, and

$$\Delta[r,\lambda(\theta)] \triangleq \frac{\log[1+\lambda(\theta)] - \log[1+r^{D_a^1(r,\theta)-D_a^2(r,\theta)}\lambda(\theta)]}{\log r} \quad . \tag{36}$$

So

$$D_a^3(r,\theta) = D_a^1(r,\theta) + \Delta[r,\lambda(\theta)] \quad . \tag{37}$$

A sign analysis of $\Delta[r,\lambda p(\theta)]$ in (36) shows that any conceivable case produces following implications :

$$\begin{aligned} D_a^1(r,\theta) \leq D_a^2(r,\theta) &\Longrightarrow D_a^1(r,\theta) \leq D_a^3(r,\theta) \leq D_a^2(r,\theta) \\ D_a^1(r,\theta) \geq D_a^2(r,\theta) &\Longrightarrow D_a^1(r,\theta) \geq D_a^3(r,\theta) \geq D_a^2(r,\theta) \quad . \end{aligned} \tag{38}$$

<u>Corollary</u> : By applying de l'Hôpital's rule in (36), we find that

$$\Delta[1,\lambda(\theta)] = \frac{[D_a^2(1,\theta) - D_a^1(1,\theta)]\lambda(\theta)}{1+\lambda(\theta)}, \tag{39}$$

resulting in the following *weighted average* equation

$$D_a^3(1,\theta) = \frac{1}{1+\lambda(\theta)}D_a^1(1,\theta) + \frac{\lambda(\theta)}{1+\lambda(\theta)}D_a^2(1,\theta). \tag{40}$$

<u>Remarks</u> :

- Notice that nothing specific has been required about T_{01} and T_{02}, nor about the way in which the subintervals of both types are distributed. Only the ratio λ of the average number of level-crossings plays a role.
- When the signal components of type 2 do not exhibit crossings of the level considered, $\lambda(\theta) = 0$. It then follows that $D_a^3(r,\theta) = D_a^1(r,\theta)$.
- This property can easily be generalized to the case of more than two merging signals.

2.3 $D_a(r,\theta)$-values for some special signals.

In this section, a few signals will be discussed that exhibit constant values of $D_a(r,\theta)$ over a large range of r, θ and a. These values will later appear as limit-values in the study of stationary normal processes.

- a. $1/f^\beta$-fractional Brownian motions.
  As was mentioned in the introduction, the fractional noises with spectrum $1/f^\beta (1 < \beta < 3)$ have zero-sets that are completely statistically self-similar. It follows that $D_a(r,\theta)$ is a constant for all a, r and θ. Moreover, from Voss [9] (see also the remarks around equations (4)-(5)), it is known that

$$D_a(r,\theta) = \frac{3-\beta}{2} = 1 - H \ . \tag{41}$$

- b. Sampling-invariant independent signals.
  Consider a discrete signal with sampling interval θ_{min}. The signs of the successive samples are outcomes of independent Bernoulli-trials, with a fixed probability p for the occurrence of one of the signs. Now take samples at distances $k\theta_{min}$ and $l\theta_{min}$, where k and l are integers. The resulting $k-$ and $l-$ subsequences are statistically similar due to the independency. Because of this, the expected number of crossings (sign-changes) is just proportional to the number of samples in the observation interval. This gives

$$\begin{aligned} D(\frac{k}{l}, l\theta_{min}) &= \frac{\log EN(T_0, l\theta_{min}) - \log EN(T_0, k\theta_{min})}{\log k/l} \\ &= \frac{\log \nu \frac{T_0}{l\theta_{min}} - \log \nu \frac{T_0}{k\theta_{min}}}{\log k/l} = 1. \end{aligned} \tag{42}$$

  (ν is a proportionality factor).
  This is true for *any* k, l. In principle, θ_{min} can be made as small as one wants. As $\theta_{min} \to 0, l\theta_{min}$ and $(k/l)\theta_{min}$ tend to evolve quasicontinuously. For these signals, independency is an invariant at any sampling period θ, hence the name used at the heading of this paragraph. The $D_a(r,\theta)$-transform of such signals is constant and equals 1 for the (r,θ)-values for which it is defined, and this for all possible values of the probability p. This probability has a one-to-one correspondence with the signal level a for a given amplitude distribution of the signal. It follows that $D_a = 1$ holds for all levels.

- c. Smoothly varying signals with minimal level crossing distance δ.
  Consider a sampling distance $\theta < \delta$, where δ is the minimal crossing distance. Then the signal can produce at most one level crossing in such a sampling interval. It follows that $EN_a(\theta) =$ constant for all $\theta < \delta$. So

$$D_a(r,\theta) = \frac{\log EN_a(\theta) - \log EN_a(r\theta)}{\log r} = 0 \tag{43}$$

  for θ such that $\max(\theta, r\theta) < \delta$

3 $D_a(r,\theta)$ for stationary normal processes.

3.1 General expressions

For a stationary normal process, the $D_a(r,\theta)$-transform can be written as a function of the *autocorrelation function* $\phi(\tau)$ of the process (so $\phi(0)=1$), using the following results which were derived in Barbé [3] :

$$EN_0(\theta) = \frac{1}{\pi\theta}\arccos\phi(\theta) \quad \text{with} \quad \arccos\phi(\theta) \in [0,\pi] \quad . \tag{44}$$

For the expected number of crossings of a nonzero *normalized* level a (normalized with respect to the signal's standard deviation), a formula was derived in [3] showing an integral function. As shown in the appendix A.1.1 (formula A1.23), that function can be transformed into the following expression featuring a series involving generalized Laguerre-polynomials :

$$EN_a(\theta) = \frac{2\sqrt{q(\theta)}}{\pi\theta}\exp(-a^2/2)\cdot\sum_{n=0}^{\infty}\frac{L_n^{(-\frac{1}{2})}(a^2/2)q^n(\theta)}{2n+1} \quad , \tag{45}$$

with

$$q(\theta) \triangleq [1-\phi(\theta)]/2. \tag{46}$$

A recursive expression for $V_n(a^2/2,\phi(\theta)) \triangleq L_n^{(-\frac{1}{2})}(a^2/2)\cdot q^n(\theta)$ is given in appendix A1.4, and makes (45) computationally interesting.

In order to clarify the meaning and usefulness of $D_a(r,\theta)$, it will be derived for a large diversity of situations using the expressions (44) and (45). From the definition (13) and from (44) we find that

$$D_0(r,\theta) = 1 + \frac{\log\arccos\phi(\theta) - \log\arccos\phi(r\theta)}{\log r} \quad . \tag{47}$$

$D_0(r,\theta)$ can be obtained by taking the limit in (47), or by invoking property 2.7 through formula (34)

$$D_0(1,\theta) = 1 + \frac{\theta}{\sqrt{1-\phi^2(\theta)}\arccos\phi(\theta)}\frac{d\phi(\theta)}{d\theta} \quad . \tag{48}$$

For an *arbitrary* constant level a, it is found that

$$D_a(r,\theta) = 1 + \frac{\log R_a(\theta) - \log R_a(r\theta)}{\log r} \quad , \tag{49}$$

with

$$R_a(\theta) \triangleq \sqrt{q(\theta)}\cdot\sum_{n=0}^{\infty}\frac{L_n^{(-\frac{1}{2})}(a^2/2)q^n(\theta)}{2n+1} \quad . \tag{50}$$

Using (34) and formula (A1.33) from the appendix, we obtain the following expression for $\tau = 1$:

$$D_a(1,\theta) = 1 + \frac{\theta}{\sqrt{1-\phi^2(\theta)}} \cdot \frac{1}{2R_a(\theta)} \exp[-\frac{a^2}{2} \cdot \frac{1-\phi(\theta)}{1+\phi(\theta)}] \frac{d\phi(\theta)}{d\theta} \quad . \tag{51}$$

Some properties about the derivatives of $D_a(r,\theta)$ with respect to the level a can be found in appendix A1.3.

3.2 Gaussian signals with asymptotic $f^{-\beta}$ power spectral behaviour.

Consider the class of Gaussian signals with correlation function

$$\phi_\nu(\tau) = \frac{1}{\Gamma(\nu-1/2)2^{\nu-3/2}} \tau^{\nu-1/2} K_{\nu-1/2}(\tau), \tag{52}$$

with $\nu > 0.5$ and $K_\nu(\tau)$ the *modified Bessel-function* (Abramowitz [12]). The corresponding spectrum-generating filter has the impulse response

$$h_\nu(t) = [\frac{2\sqrt{\pi}}{\Gamma(\nu)\Gamma(\nu-1/2)}]^{1/2} t^{\nu-1} e^{-t}. \tag{53}$$

The associated power spectral density is given by

$$S_\nu(\omega) = \frac{2\sqrt{\pi}\Gamma(\nu)}{\Gamma(\nu-1/2)} \frac{1}{(1+\omega^2)^\nu} \quad . \tag{54}$$

This spectrum behaves asymptotically as $\omega^{-\beta} = \omega^{-2\nu}$. For $0.5 < \nu < 1.5$, these signals exhibit microscopic fractional Brownian motion behaviour. Figure 5 shows the zero-level dimensionality $D_0^\nu(1,\theta)$ for different values of $\beta = 2\nu$.

For large values of the sampling period θ, $D_0(1,\theta)$ evolves asymptotically to the value 1. This should be no surprise as the fact that $\phi_\nu(\tau)$ tends to 0 for large τ, makes these signals asymptotically *sampling-invariant independent* (see section 2.3).

For small values of θ, $D_0^\nu(1,\theta)$ tends to a limit value. As shown in appendix 2, this limit value is given by the fractal dimension of the zero-set of the fractional Brownian motion to which the signals under consideration tend at these microscopic scales :

$$\lim_{\theta \to 0} D_0^\nu(1,\theta) = \frac{3-\beta}{2} = 1.5 - \nu \text{ for } \nu \leq 1.5 \quad . \tag{55}$$

In view of the discussion in section 2.3.a, this result is not so unexpected. It actually means that the considered processes are fractal processes with a fractal

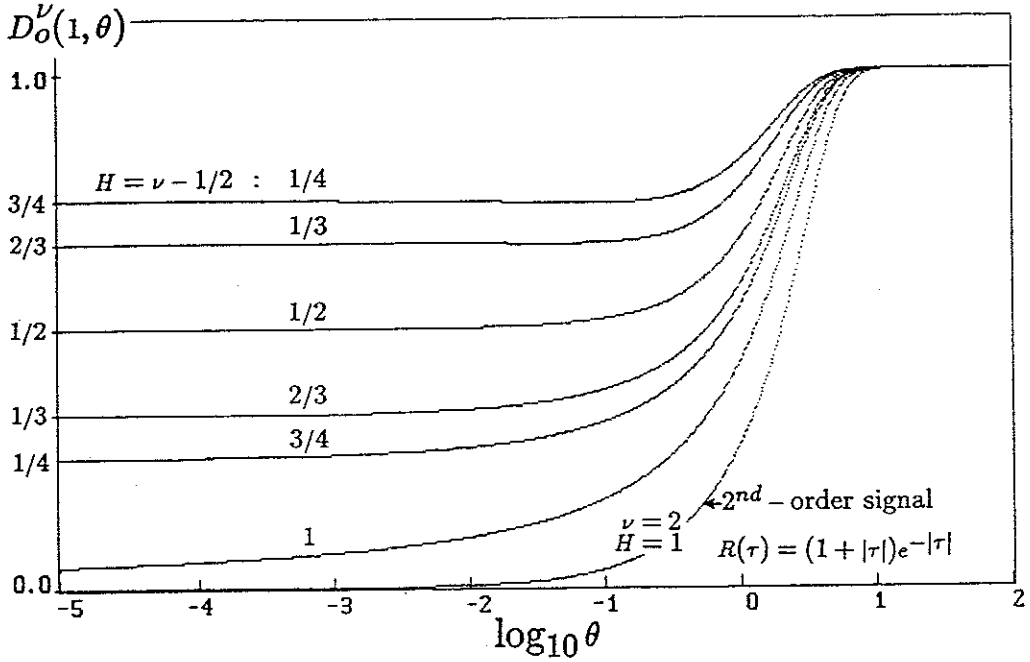


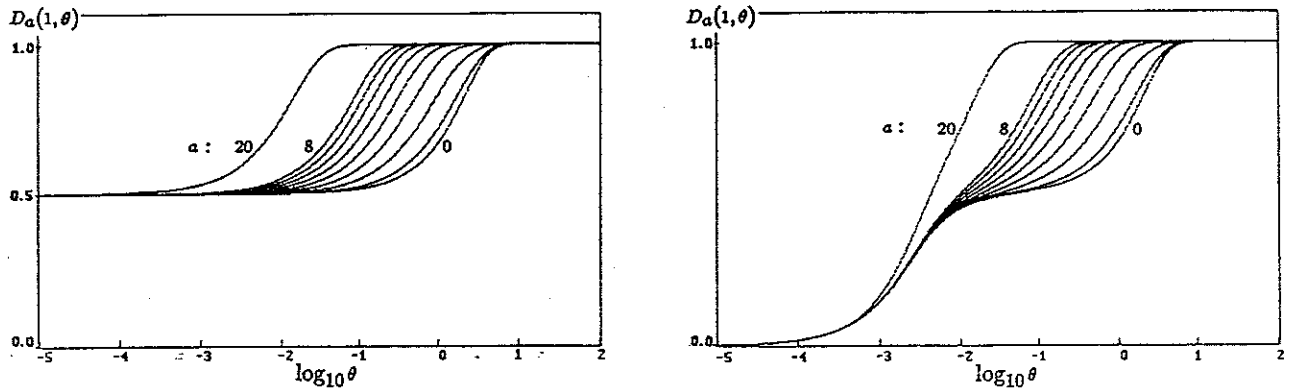
Figure 5: $D_o^\nu(1,\theta)$ for signals with spectrum $(1+\omega^2)^{-\nu}$.

dimension given by (55).
For $\nu \geq 1.5$, the signals with correlation function (52) become mean square differentiable, and as shown in appendix 2,

$$\lim_{\theta \to 0} D_0^\nu(1,\theta) = 0 \text{ for } \nu \geq 1.5 \quad . \tag{56}$$

This result is related to the one obtained in section 2.3.c for smoothly varying signals. As a matter of fact, the processes in the class represented by (53) with $\nu \geq 1.5$ have continuous derivatives with probability one, as they satisfy condition (9.5.5) in Cramér-Leadbetter [6]. That the limit in (56) is only reached asymptotically (on logaritmic θ-scale), and does not hold for all θ smaller than some $\theta_{\max} \neq 0$, is due to the fact that arbitrary small distances δ between successive level-crossings may occur.

The limiting values that emerged above remain the same when values of $r \neq 1$ and/or level values $a \neq 0$ are considered. This is a consequence of the derivative properties A1.41 and A1.42 from appendix 1, and is illustrated in figure 3 for $r \neq 1$, and in figure 6 for $a \neq 0$.
The behaviour of signals at high frequencies depends on the behaviour of the correlation function $\phi(\tau)$ in the neigborhood of $\tau = 0$. Figure 7 shows the classification of the signals according to the conditions on the first and second derivatives of $\phi(\tau)$ at $\tau = 0$. Four different categories seem to emerge.



a. $\phi(\tau) = \exp(-|\tau|)$

b. $\phi(\tau) = \frac{1}{1-\beta}[\exp(-|\tau|) - \beta\exp(-|\tau|/\beta)]$
$(\beta = 0.001)$

Figure 6: Level dependence of $D_a(1,\theta)$ for two different processes.

signal category	Behaviour of power spectrum for large ω : $\propto \omega^{-\beta} = \omega^{-2\nu}$ ν	H $D_a(r,0) = 1 - H$	Behaviour of signal covariance $\phi(\tau)$ at $\tau = 0$: $1 - \mu\tau^{2H} + o(\tau^{2H})$	Behaviour of $\dot{\phi}(\tau)$ at $\tau = 0$	Behaviour of $-\ddot{\phi}(\tau)$ at $\tau = 0$	Nature of singularity in the spectrum-generating filter (shown at $t = 0$: $O(t^{\nu-1})$)
non-differentiable *I*	$0.5 < \nu < 1$	$H = \nu - 1/2$ $0 < H < 0.5$ $0.5 < D < 1$			Dirac-delta	$\in L_2$
non-differentiable *II*	$\nu = 1$	$H = \nu - 1/2$ $H = 0.5$ $D = 0.5$	$\mu = -\dot{\phi}(o^+)$			
non-differentiable *III*	$1 < \nu \leq 1.5$	$H = \nu - 1/2$ $0.5 < H \leq 1$ $0 \leq D < 0.5$				
differentiable *IV*	$\nu > 1.5$	$H = 1$ $D = 0$	$\mu = \frac{1}{2}\ddot{\phi}(o)$			

Figure 7: Classification of signals according to their microscopic (high-frequency) behaviour.

Observe that the categories II and IV represent the most common signal models (all signals with rational spectrum belong to these categories), and they have as limiting values $D_a(r,0) = 0.5$ and $D_a(r,0) = 0$ respectively. Signal models of the categories I and III are quiet uncommon in the engineering literature. However, many *physical* signals of interest seem to belong to the categories I and III (Mandelbrot and Van Ness [7]). Also the category of so-called 1/f-noises (Schuster [13], Voss [9]) which represent noises with power spectrum $f^{-\beta}$ where $\beta \in (0.5, 1.5)$ (this β-interval depends on the authors), partially belongs to category I. When $\beta \leq 1$, the corresponding signals no longer belong to the class of stationary signals under study here.

So far, the $D_a(1,\theta)$-transform can give an idea about the interval $(0,\theta_c]$ for which the very microscopic statistical self-similarity of the level crossings under rescaling remains quasi-constant. This will be named the *microcharacteristic interval*. Recall that for the fractional Brownian motions, the following scaling property holds exactly over all time scales

$$EN_a(\theta) = r^{D^o} EN_a(r\theta). \tag{57}$$

D^o is the fractal dimension of the corresponding level-crossing set. For the signals under consideration here, $D^o = D_a(r,0) = \lim_{\theta \to 0} D_a(r,\theta)$, and by definition, we have

$$EN_a(\theta) = r^{D_a(r,\theta)} EN_a(r\theta). \tag{58}$$

The microcharacteristic interval $(0,\theta_c]$ is then determined by the condition that the relative error on this relationship when considering the level crossings as coming from the exact fractional Brownian motion instead of from the signal actually considered, should be sufficiently small, i.e.

$\forall \theta \in (o,\theta_c]$ and $\forall r \in (o, \frac{\theta_c}{\theta})$:

$$r^{D^o} = (1 + \delta_{r,\theta}) r^{D_a(r,\theta)}, \text{with } |\delta_{r,\theta}| \leq \delta_{\max}. \tag{59}$$

$\delta_{\max}$ is the maximal relative inaccuracy to be tolerated, and imposes a uniform upper bound on $\delta_{r,\theta}$.

Taking logarithms of both sides and using property 2.3 (formula 22) transforms (59) into

$$\log(1 + \delta_{r,\theta}) = \int_{\log r\theta}^{\log \theta} [D_a(1,\zeta) - D^o] d\log\zeta \quad . \tag{60}$$

It follows that $(o, \theta_c(\delta_{\max})]$ should be selected as the maximal $(o, \theta]$-interval for which $D_a(1, \zeta)$ stays sufficiently close to D^o in the following sense :

$$\sup_{\substack{0 < r < 1 \\ \theta \in (o, \theta_c]}} \left| \int_{\log r\theta}^{\log \theta} [D_a(1, \zeta) - D^o] d \log \zeta \right| \leq \log(1 + \delta_{\max}) \simeq \delta_{\max} \qquad (61)$$

(The rightmost approximation requires that $\delta_{\max}$ is sufficiently small).
Notice that (61) is a much stronger condition than just $|D_a(1, \theta) - D^o| < \varepsilon_{\max}$ for some small $\varepsilon_{\max}$ and $\forall \theta \in (0, \theta_c]$. In fact, (59) and (61) are also equivalent to a selection of a maximal θ_c such that

$$\forall \theta \in (0, \theta_c] \text{ and } \forall r < 1 : |D_a(r, \theta) - D^o| \leq \frac{\log(1 + \delta_{\max})}{|\log r|} \simeq \frac{\delta \max}{|\log r|} \ . \qquad (62)$$

In appendix 2 it is shown in formula (A2.19) that for the *zero-level* crossings, and for sufficiently small θ :

$$D_o(r, \theta) - D^o \simeq \alpha \frac{1 - r^\chi}{\log r} \theta^\chi, \qquad (63)$$

with α and χ signal-specific parameters. Combined with (62), it follows that the upper bound of the microcharacteristic interval for zero-level crossings is given by

$$\theta_c = (\frac{\delta_{\max}}{\alpha})^{1/\chi} \ . \qquad (64)$$

The expressions (63-64) are valid only for θ_c sufficiently small, and this is tied to $\delta_{\max}$ being sufficiently small. For larger $\delta_{\max}$ or θ_c in (64), one should use the nonapproximated expression for $D_a(r, \theta)$ in condition (62). Expressions for θ_c according to (64) for different signals are given in appendix 3. Figure 8 shows this θ_c for some signals and for $\delta_{\max} = 0.01$. Observe the discontinuity for the Bessel-type correlated signals. Also notice that the microcharacteristic interval for the Besseltype signals vanishes for $\mu \to 0.5^+$ and for $\mu \to 1.5^-$ (in fact, it is very small for $0.5 < \mu < 0.65$ and for $1.25 < \mu < 1.5$).
Consider fig. 9, representing $D_o(1, \theta)$ for the signal with correlation function $\phi(\tau) = \frac{1}{1-\beta}(e^{|\tau|} - \beta e^{-|\tau|/\beta})$ for $\beta = 10^{-7}$. This signal corresponds to a slightly smoothed version of the exponentially correlated signal. For $\theta > \theta_{\min}$, the $D_o(1, \theta)$ curves for both signals practically coincide : at these sampling scales, the difference between the two signals becomes unnoticeable. Also, $D_o(1, \theta)$ remains very close to $D^o = 0.5$ in the interval $[\theta_{\min}, \theta_{\max}]$. It means that the smoothed signal has the same approximate self-similarity as the non-smoothed signal in this finite interval. Also, for a $\theta \in [\theta_{\min}, \theta_{\max}]$, the *minimal* scaling

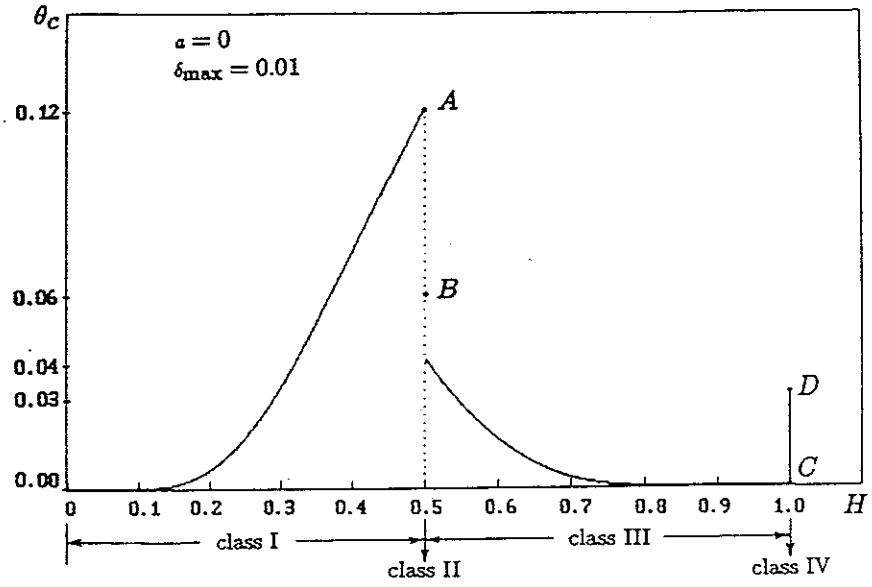


Figure 8: The upper bound θ_c for the microcharacteristic interval of several signals (related to the zero-level, $\delta_{\max} = 0.01$). Solid line : for the Bessel-type correlation functions (eqn. 52, $H = \nu - 0.5$).
$A : \phi(\tau) = \max(o, 1 - |\tau|)$; $B : \phi(\tau) = \exp(-|\tau|)$.
$CD : \phi(\tau) = \frac{1}{1-\beta}[\exp(-|\tau|) - \beta \exp(-|\tau|/\beta)], \beta \in (o, 1); [C : \beta \to o, D : \beta \to 1]$.

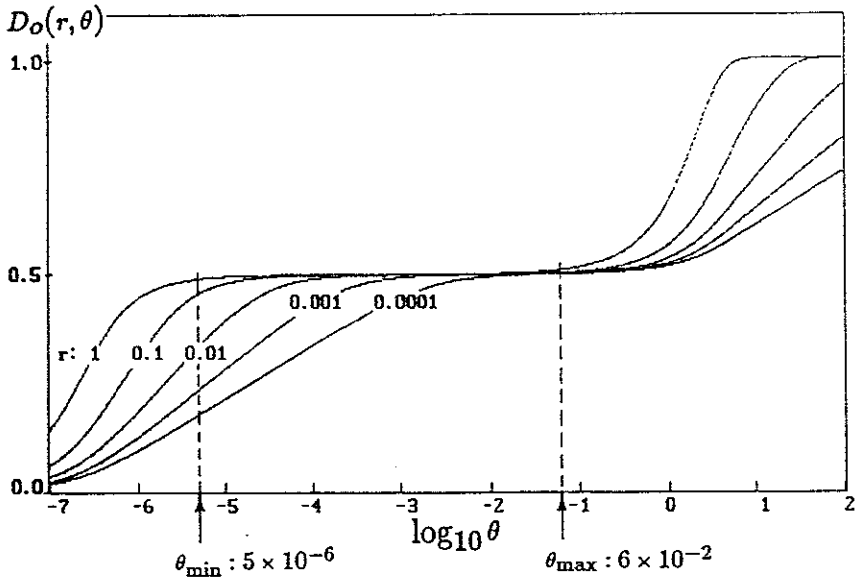


Figure 9: $D_o(r, \theta)$ for the signal with correlation function
$\phi(\tau) = \frac{1}{1-\beta}(e^{|\tau|} - \beta e^{|\tau|/\beta}), \beta = 10^{-7}$. $(\theta_{\min}, \theta_{\max})$ is the interval for which the signal shows approximately the same microcharacteristic behaviour ($\delta_{\max} \simeq 0.01$) as the Brownian motion ($D^o = 0.5$).

factor r that can be considered without breaking this self-similarity will now depend on θ, namely $r_{\min}(\theta) = \theta_{\min}/\theta$. Also $r_{\max}(\theta) = \theta_{\max}/\theta$.

These examples urge to define the following generalized distance-measure and related closeness-concept between two signals. Consider two signals $x(t)$ and $y(t)$ with respective scaling-dimension transform $D_a^x(r,\theta)$ and $D_a^y(r,\theta)$. The *D_a-distance* $d_{D_a}^{x,y}(\theta_1,\theta_2)$ between these signals in an interval $[\theta_1,\theta_2]$ is given by

$$d_{D_a}^{x,y}(\theta_1,\theta_2) = \sup_{\substack{\theta_1/\theta < r < \theta_2/\theta \\ \theta_1 \le \theta \le \theta_2}} \left| \int_{\log r\theta}^{\theta} [D_a^x(1,\zeta) - D_a^y(1,\zeta)] d\log\zeta \right| \quad . \tag{65}$$

The signals are said to be *$D_a(\delta_{\max})$-close in the interval* $[\theta_1,\theta_2]$ when

$$d_{D_a}^{x,y}(\theta_1,\theta_2) \le \log(1+\delta_{\max}) \simeq \delta_{\max} \quad . \tag{66}$$

The direct translation of (59), gives an alternative but equivalent form to (66) for $D_a(\delta_{\max})$-closeness in $[\theta_1,\theta_2]$:

$$\forall\theta \in [\theta_1,\theta_2] \text{ and } \forall r \in [\frac{\theta_1}{\theta},\frac{\theta_2}{\theta}] : |D_a^x(r,\theta) - D_a^y(r,\theta)| \le \frac{\log(1+\delta_{\max})}{|\log r|} \simeq \frac{\delta_{\max}}{|\log r|} \; . \tag{67}$$

The fact that $D_a(r,\theta) = D_a(r^{-1},r\theta)$ allows the restrictive interval on r to be replaced by $[\frac{\theta_1}{\theta},1]$ or by $[1,\frac{\theta_2}{\theta}]$.

As such, and in analogy, one could argue that it is also possible to find a θ_c-value from the very power spectrum $S(f)$ of the signal itself. Take e.g. $\theta_c = f_c^{-1}$, where f_c would be the minimal frequency from which on $S(f)$ stays "close enough" to its asymptote $f^{-\beta}$. However, dependent on the particular distance-measure, one finds contradictory evolutions for θ_c as dependent on ν for the Bessel-type correlated signals. Moreover, the characteristic discontinuous separation of the four categories as it emerges from the scaling dimensionality analysis and as shown in figure 8 is totally absent when considering the spectrum. Besides, although equations (63) and (64) relate to zero-level crossings, the general condition (62) will produce a θ_c that also depends on the level a. The microcharacteristic level-crossing behaviour for the higher levels will extend over a smaller time scale, as is reflected in the observed left-shift of the $D_a(1,\theta)$-curves for increasing level a. This kind of level-dependent information is completely absent in the mere power spectrum.

The next section will go one step further by relating the sampling resolution to a resolution in amplitude.

4 Level-crossing activity of blurred signals (stationary, gaussian).

4.1 The background idea

The theoretical continuous-time description of a signal as given by its covariance function or power spectrum, contains all signal information with an infinitely high resolution. This is what makes the direct application of Rice's formula for the assessment of the level-crossing rate practically useless. Recall that we are looking for a means to get rid of too much microscopic detail. The way in which images of the signals are produced in this paper already hides microscopic details because of the pixel-based representation with limited resolution in time and amplitude. But, what time and -amplitude scales are relevant hereby ? Another way to remove unnecessary detail, and in which pixel-based representations can be approximately imbedded, is to look at the (infinitely)-high resolution pictures in a defocussed way. The higher the degree of defocussing, the more details will disappear : clusters of close level-crossings with small peaks will merge into one bigger macroscopic crossing. The macroscopic level-crossing activity of a signal can be assessed by looking at the macroscopic level crossings of such a defocussed signal, whereby the result will depend on the degree of defocussing, which should preferably be controllable. Defocussing or blurring of a signal with a varying degree can be done mathematically in a nice way. Just superimpose a very fast signal on the original one in an additive and independent way. An example showing blurred versions of the images from fig. 1a is given in figure 10.

The degree of blurring will then depend on the ratio of the amplitudes of the blurring signal and of the original signal, and can be varied. In the case of the normally distributed blurring signals that will be considered here for reasons of analytical tractability, the amplitude is potentially unbounded. However, the intensity of the blur decreases for larger amplitudes, according to the gaussian density function. So the effective blurring range can be considered as proportional to the standard deviation σ_b of the blurring signal. The ratio of this range over the standard deviation σ_x of the original signal $x(t)$ will be called the blurring factor $f_{b,\alpha}$:

$$f_{b,\alpha} \triangleq \alpha \frac{\sigma_b}{\sigma_x}. \tag{68}$$

α is a factor to be agreed upon, but $\alpha = 3 \ldots 4$ seems an acceptable value as the intensity seems to fade clearly outside the interval $(-\alpha\sigma_b, +\alpha\sigma_b)$. However, α may also be specific to the application, and that's why only the ratio $f_b \triangleq \sigma_b/\sigma_x$ will be mentioned as blurring factor in the sequel.

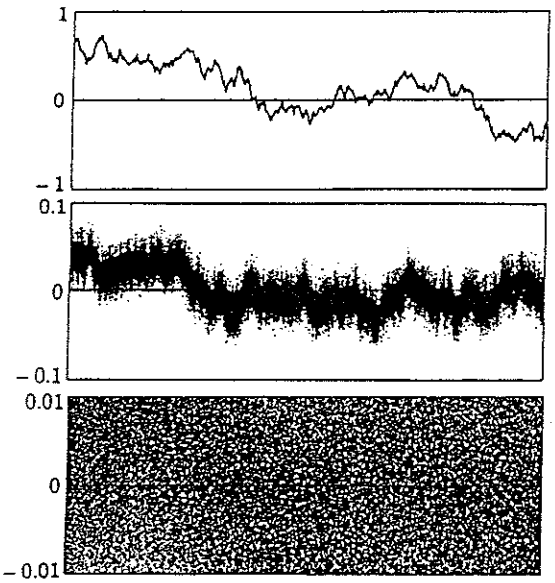


Figure 10: Blurred versions of the signals in figure 1a (blurring factor $f_b = 0.01$).

4.2 The $D_a(1,\theta)$-transform of blurred signals

Consider an arbitrary stationary gaussian signal $b(t)$ with autocorrelation function $\phi_b(\tau)$, for which $\lim_{\tau\to\infty}\phi_b(\tau) = 0$. Its infinitely time-compressed form : $\lim_{\gamma\to\infty} b(\gamma t)$, will be called an *extremely fast signal* and will be denoted by $b_\infty(t)$. The correlation function of such an extremely fast signal looks very degenerate : it is zero everywhere, except for $\tau = 0$ where it equals σ_b^2. This is true whatever the particular form of $\phi_b(\tau)$. In fact, any extremely fast signal is a sampling-invariant independent signal, and its D-transform equals 1 for all θ. When a signal $x(t)$ with autocorrelation function $\phi_x(\tau)$ is blurred with such an extremely fast signal by superposing the latter on the former in an independent way, a *blurred* signal $xb_\infty(t)$ is obtained, with variance and autocorrelation function

$$\sigma^2_{xb_\infty} = \sigma_x^2 + \sigma_b^2 = \sigma_x^2(1+f_b^2) \quad , \tag{69}$$

$$\begin{aligned} \phi_{xb_\infty}(\tau) &= 1 \quad \text{for } \tau = 0 && (70)\\ &= \frac{1}{1+f_b^2}\phi_x(\tau) \quad \text{for } \tau \neq 0 \ . && (71) \end{aligned}$$

Expression (71) is the one to be used in the derivation of $D_a(1,\theta)$ through equations (48) and (51).

The blurring signal being Gaussian and extremely fast, it exhibits an infinite number of level crossings in any nonzero interval, at any level. Hence, this will also be the case for the blurred signal $xb_\infty(t)$ itself. It seems natural then to expect that the $D_o^{xb_\infty}(1,\theta)$-curve will coincide with the $D_o^{b_\infty}(1,\theta) \equiv 1$ curve. However, this is not so, as illustrated by the generic examples of figure 11.

Observe that within the microcharacteristic θ-interval, the $D_a^{xb_\infty}(1,\theta;f_b)$-curves for different values of the blurring factor f_b are approximately shifted versions of each other. This is a consequence of the fact that the signal $x(t)$ when blurred by $b_\infty(t)$, and the signal $x(\rho t)$ when blurred by $b'_\infty(\rho t)$ with $f'_b = \rho^H f_b$ are statistically self-affine, i.e.

$$xb'_\infty(\rho t) \stackrel{s}{\simeq} \rho^H xb_\infty(t). \tag{72}$$

Indeed, this follows from the approximate self-affinity of $x(t)$ in the microcharacteristic interval, implying that $x(\rho t) \stackrel{s}{\simeq} \rho^H x(t)$, and from the relationship $b'_\infty(\rho t) \stackrel{s}{\simeq} \rho^H b_\infty(t)$. The corresponding self-similarity of the level-crossing sets then entails

$$D_a^{xb_\infty}(1,\theta;f_b) \simeq D_a^{xb_\infty}(1,(f'_b/f_b)^{1/H}\theta;f'_b)\ . \tag{73}$$

On the logarithmic θ-scale shown in the figures, it means that $D^{xb_\infty}(1,\theta;f_b)$ and $D^{xb_\infty}(1,\theta;f'_b)$ are shifted over a distance $\frac{1}{H}\log(f'_b/f_b)$.

Three zones can be distinguished in these graphs (fig. 12). The location of the boundaries between them depends on the particular value of the blurring factor f_b.

<u>Zone 1</u> : $\theta \geq \theta_M$.

This is the zone where $D_a^{xb_\infty}(1,\theta)$ is rather close to $D_a^x(1,\theta)$. For a given $\theta \geq \theta_M$, the amplitude of the blurring signal is so small that it does not practically affect the level-crossing behaviour of $x(t)$ at the time scale considered. The tremendous level-crossing behaviour of the extremely fast blurring signal is almost undetectable at this sampling rate. For sufficiently small f_b, this domain overlaps a part I_μ of the microcharacteristic interval of $x(t)$. In this overlap, the standard deviation of the blurring signal is much smaller than the magnitude of the increment of $x(t)$ at the time distances considered, i.e.

$$\sigma_b << \sigma_x\sqrt{2\mu}\theta^H \ \text{ or } \ f_b << \sqrt{2\mu}\theta^H\ . \tag{74}$$

It will be said that the original signal $x(t)$ and its blurred version are *indistinguishable* with respect to their macroscopic level-crossing behaviour (MLC-indistinguishable), for time units (sampling-distances) larger than θ_M. In analogy with the way in which the upper limit of the microcharacteristic interval

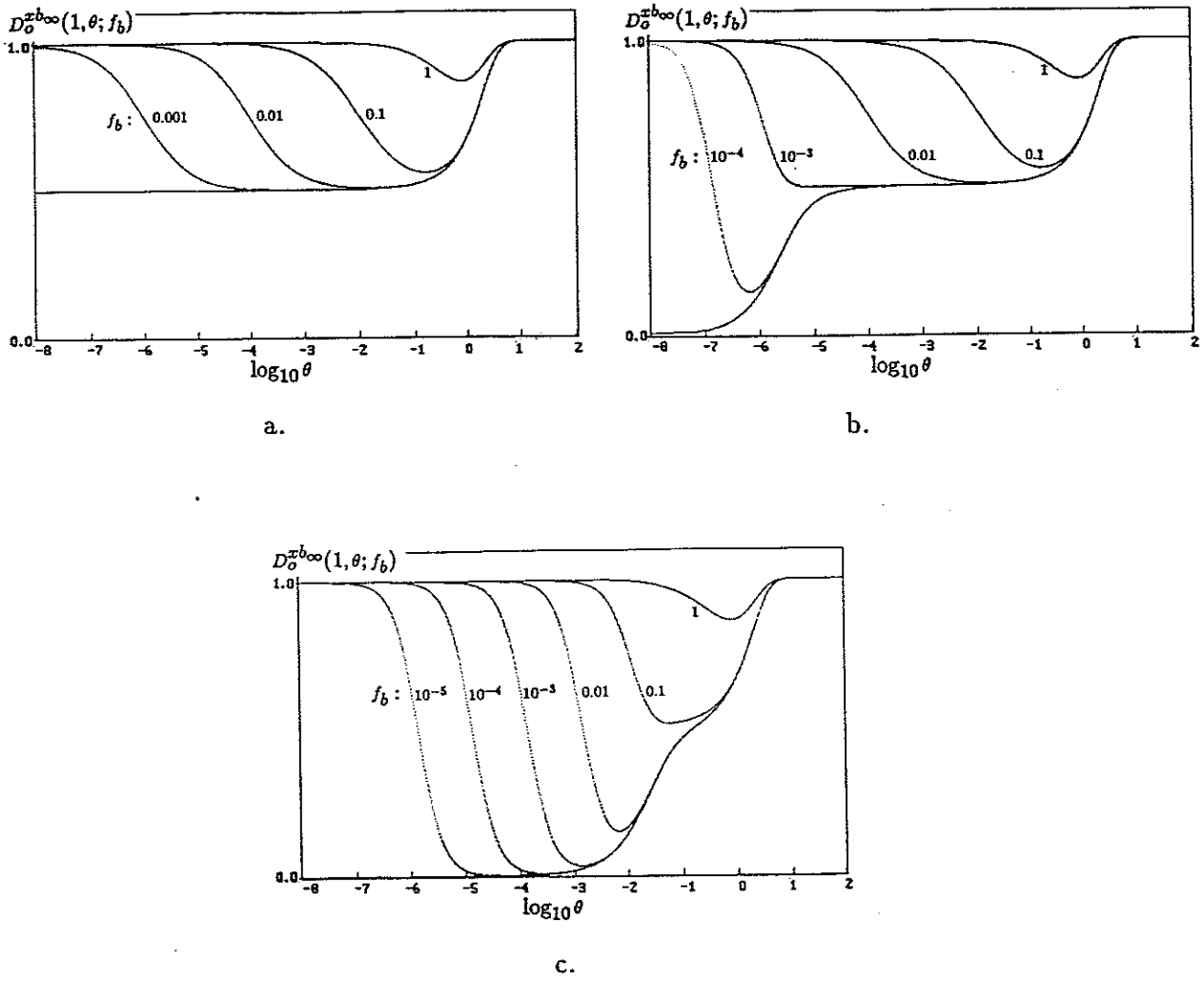


Figure 11: The $D_o(1,\theta)$-transform for blurred signals.
a. for signal with correlation function $\phi(\tau) = \exp(-|\tau|)$.
b. for signal with correlation function $\phi(\tau) = \frac{1}{1-\beta}[\exp(-|\tau|) - \beta\exp(-|\tau|/\beta)], \beta = 10^{-6}$
c. as b., but with $\beta = 0.01$.

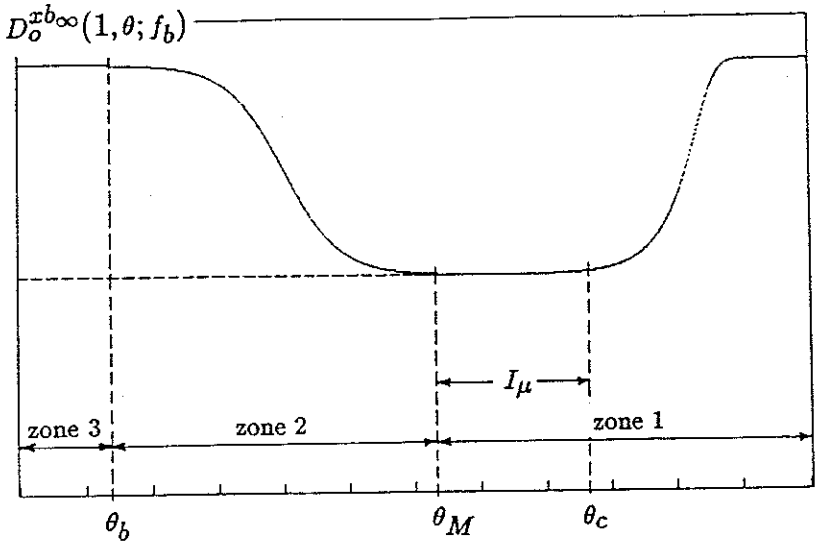


Figure 12: θ-trichotomy of the $D_a^{xb_\infty}(1,\theta)$-transform of a signal blurred by an extremely fast signal.

(section 3, eqn. 62) was found, one can define $\theta_M(f_b, \delta_{\max}; a)$ as the minimal value of θ for which $xb_\infty(t)$ and $x(t)$ are $D_a(\delta_{\max})$-close in $[\theta_M, \infty]$ (cf. definition (66)).

Recall that this is equivalent to θ_M being the minimal value such that

$$\forall \theta \geq \theta_M \text{ and } \forall r > 1 : |D_a^{xb_\infty}(r,\theta;f_b) - D_a^x(r,\theta;f_b)| \leq \frac{\log(1+\delta_{\max})}{|\log r|} \quad . \quad (75)$$

(75) allows θ_M to be found from a set of curves plotting $\log|D_a^{xb_\infty}(r,\theta;f_b) - D_a^x(r,\theta;f_b)|$ versus $\log r$ with θ as parameter. Figure 13 shows θ_M as a function of f_b for a few types of signals, and for different levels. For signals with monotone non-increasing correlation functions, it has been observed that θ_M is obtained by considering condition (75) for $r \to \infty$. For $a = 0$, this is equivalent to $\arccos[\phi(\theta_M)/(1+f_b^2)] \leq (1+\delta_{\max})\arccos\phi(\theta_M)$, which fixes $\phi(\theta_M)$ rather than θ_M. This is no longer the case when the autocorrelation function has increasing parts. θ_M can even be discontinuous in these cases, as the example in figure 13b shows.

Zone 2 : $\theta_b \leq \theta \leq \theta_M$.

When θ becomes smaller than θ_M, there are some level-crossings of $x(t)$ in whose neighbourhood $\sigma_b = f_b\sigma_x$ becomes of the same order as, or even exceeds the natural range of variation of $x(t)$ over θ (i.e. inequality 74 is no longer satisfied). *In these neighbourhoods*, the signal $x(t)$ becomes dominated by the blurring signal, hence it is found there that the scaling-dimension equals $D_a^{b_\infty}(1,\theta) = 1$. In the intervals *outside* these $b_\infty(t)$-dominated neighbourhoods, the level-crossings of $xb_\infty(t)$ are the same as those of $x(t)$ at the sampling distance θ under consideration (a sufficiently high slope at these crossings seems to be

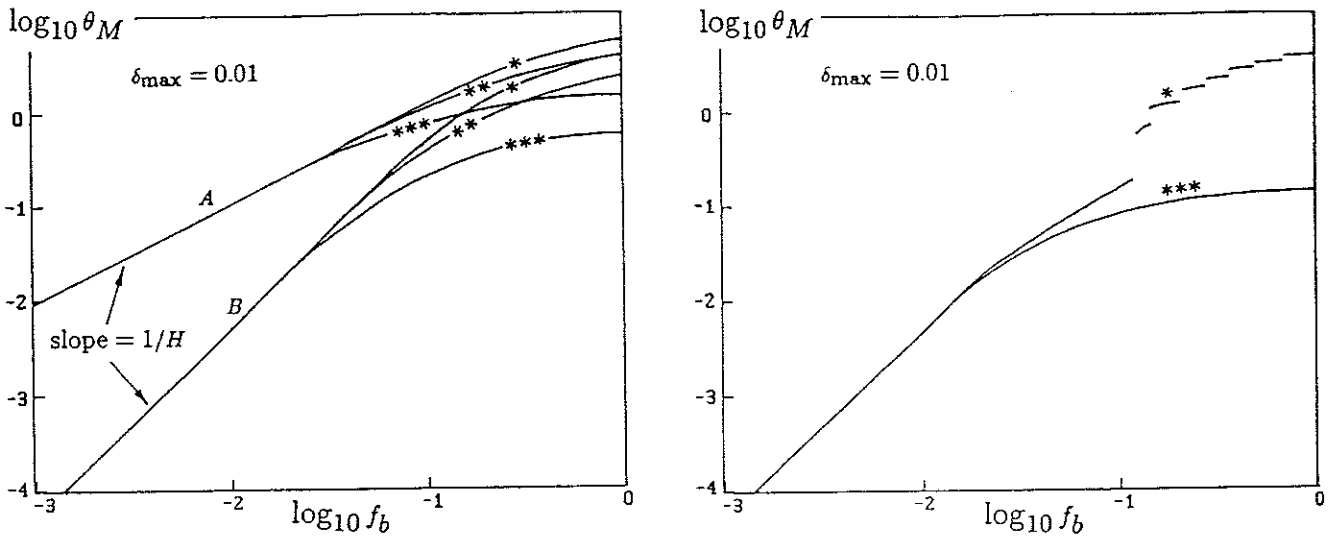


Figure 13: The lower bound θ_M of the macrocharacteristic interval as a function of the blurring factor f_b, with $\delta_{\max} = 0.01$.
a. $A : \phi(\tau) = \frac{1}{1-\beta}[\exp(-|\tau|) - \beta \exp(-|\tau|/\beta)], \beta = 0.9; B : \phi(\tau) = \exp(-|\tau|)$
b. $\phi(\tau) = \exp(-|\tau|)\cos(2\pi\tau)$; * : $a = 0$, ** : $a = 2$, *** : $a = 5$

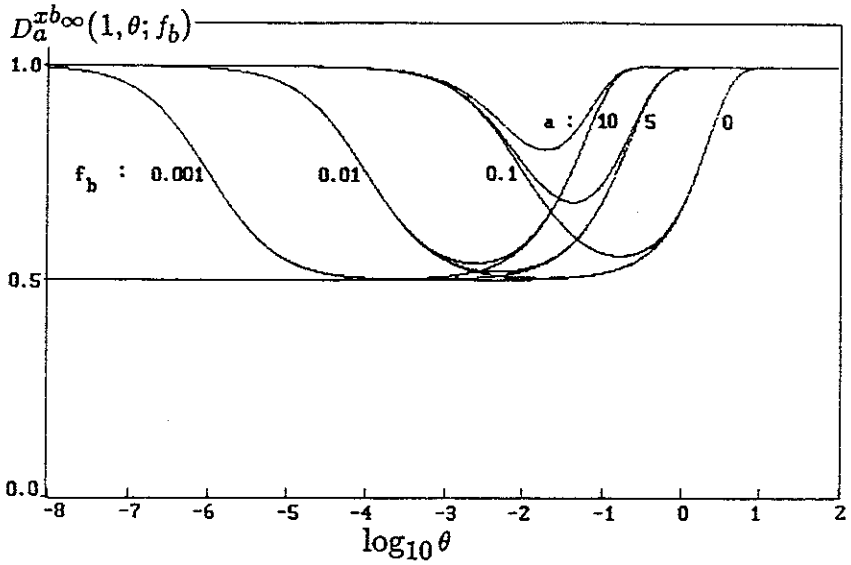


Figure 14: Level-dependence of $D_a(1,\theta;f_b)$ for blurred versions of a signal with $\phi(\tau) = \exp(-|\tau|)$.

the condition). So, it is found here that the scaling dimension equals $D_a^x(1,\theta)$. Observe from figure 14, how $D_a^{xb_\infty}(1,\theta)$ in this zone is quasi-independent of the level a. Only the size of the microcharacteristic interval varies with a.

It follows from the merging property 2.8, that the resulting overall scaling-dimension is the weighted average of $D_a^{b_\infty}(1,\theta) = 1$ and of $D_a^x(1,\theta)$ as given by formula 40. As a matter of fact, this merging property works over all three zones, but its effect is most striking in zone 2. Formula 40 allows to derive $\lambda(\theta;f_b)$, the ratio of the expected number of crossings due to $b_\infty(t)$ and contributing to $D_a^{b_\infty} = 1$, and the expected number of crossings contributing to D_a^x :

$$\lambda_a(\theta;f_b) = \frac{D_a^{xb_\infty}(1,\theta;f_b) - D_a^x(1,\theta;f_b)}{D_a^{b_\infty}(1,\theta;f_b) - D_a^{xb_\infty}(1,\theta;f_b)} \quad . \tag{76}$$

Invoking (48) and (71) transforms (76) into

$$\lambda_o(\theta;f_b) = \frac{\sqrt{(1+f_b^2) - \phi^2(\theta)}\arccos\frac{\phi(\theta)}{1+f_b^2}}{\sqrt{1-\phi^2(\theta)}\arccos\phi(\theta)} - 1 \quad . \tag{77}$$

Observe that $\lambda_o(\theta;f_b)$ only depends on θ in an implicit way : $\phi(\theta)$ is the relevant factor. The following approximations emerge :

- f_b small $: \lambda_o(\phi;f_b) \simeq [\frac{1}{1-\phi^2} + \frac{\phi}{\sqrt{1-\phi^2}\arccos\phi}]f_b^2$ (78)
- θ large (ϕ small) : $\lambda_o(\theta;f_b) \simeq f_b^2$ (79)

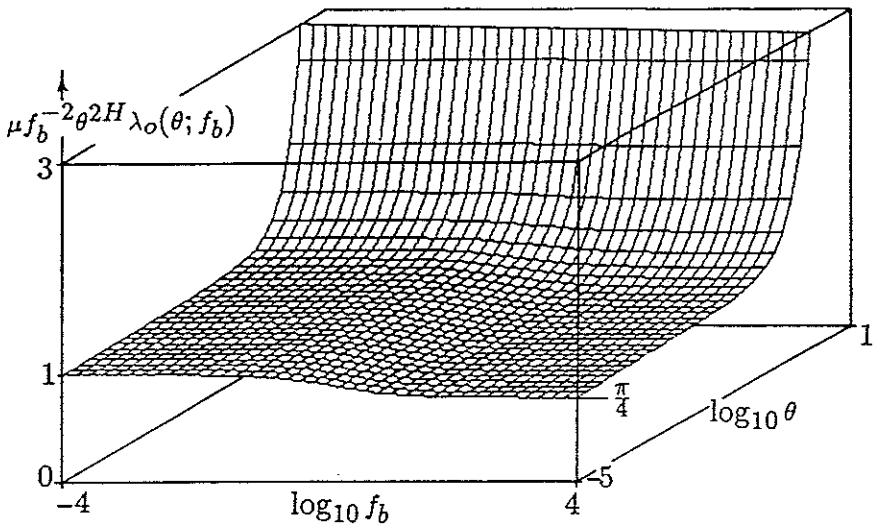


Figure 15: Plot of $\mu f_b^{-2}\theta^{2H}\lambda_o(\theta; f_b)$ for signal with $\phi(\tau) = \exp(-|\tau|)$.

- θ small $(\phi \to 1)$ and f_b small $: \lambda_o(\theta; f_b) \simeq \frac{1}{\mu} f_b^2 \theta^{-2H} (\simeq \frac{f_b^2}{1-\phi})$ (80)
  $(\mu, H$ from equation $A2.1)$
- θ small $(\phi \to 1)$ and f_b large $: \lambda_o(\theta; f_b) \simeq \frac{\pi}{4\mu} f_b^2 \theta^{-2H} (\simeq \frac{\pi}{4} \frac{f_b^2}{1-\phi})$ (81)

Figure 15 shows a generic example in which $\mu f_b^{-2}\theta^{2H}\lambda_o(\theta; f_b)$ is plotted against $\log\theta$ and $\log f_b$. Observe from this figure, and from the approximation (78-81) that this normalized value of λ_o for a fixed f_b is quasi-constant as long as θ belongs to the microcharacteristic interval. This quasi-constant value equals 1 for f_b-values that are sufficiently small to provide in an overlap between zone 1 and the microcharacteristic interval (i.e. I_μ is not empty). For f_b sufficiently large, this constant becomes equal to $\pi/4$.

Zone 3 : $\theta \leq \theta_b$

This is the zone where the sampling distance has become so small, that almost all level-crossings originate from the blurring signal. Hence it is no surprise that here $D_a^{xb_\infty}(1, \theta; f_b) \simeq D_a^{b_\infty}(1, \theta; f_b) = 1$. The original signal is practically undetectable for θ-values in this zone. θ_b can be considered as the maximal value $\theta_b(f_b, \delta_{\max}; a)$ for which the signals $x(t)$ and $xb_\infty(t)$ are $D_a(\delta_{\max})$-close in $(o, \theta_b]$, i.e.

$$\forall \theta \leq \theta_b \text{ and } \forall r < 1 : |1 - D_a^{xb_\infty}(r, \theta; f_b)| \leq \frac{\log(1 + \delta_{\max})}{|\log r|} \quad . \tag{82}$$

4.3 Selecting proper time- and amplitude resolutions for the discrete representations of signals

First, consider the sum of two random signals $x(t)$ and $y(t)$. The places where $x(t)+y(t)$ crosses a certain level a are the same as those where $x(t)$ crosses the randomly varying level $a-y(t)$. This implies that $D_a^{x(t)+y(t)}(r,\theta) = D_{a-y(t)}^{x(t)}(r,\theta)$. When $y(t)$ has zero mean, it is statistically equivalent to $-y(t)$. Hence

$$D_{a-y(t)}^{x(t)}(r,\theta) = D_{a+y(t)}^{x(t)}(r,\theta) \ .$$

With $y(t) = b_\infty(t)$, this translates into

$$D_a^{x(t)+y(t)}(r,\theta) = D_a^{xb_\infty}(r,\theta;f_b) = D_{ab_\infty}^{x}(r,\theta;f_b) \ . \tag{83}$$

Now, consider the pixel-based representation of the signal $x(t)$ (figure 16). Both time and amplitude are discretized. Time is discretized through *sampling*, at a distance θ_d, where time-pixel k_d represents the discrete time moment $k_d\theta_d$. It can be said that the time resolution is θ_d. The amplitude however is discretized by *quantization*. The pixelvalue v_d to be selected at moment $k_d = \theta/\theta_d$ is given by

$$(v_d - \frac{1}{2})\rho_d \leq x(k_d\theta_d) < (v_d + \frac{1}{2})\rho_d, \tag{84}$$

where ρ_d is the resolution or discrete unit for the amplitude. It is clear that a good discrete signal representation $x_d(k_d,\rho_d)$ should be sufficiently close to the original continuous time signal. From the context of discourse, it should be no surprise that the proposed closeness here will be the closeness in scaling behaviour for the level-crossings. Or : $D_{a_d}^{x_d}(1,k_d\theta_d) = D_{a_d}^{x}(1,k\theta_d)$ should be close to $D_a^x(1,k_d\theta_d)$, in D_a-distance sense (cf. definitions 65, 66). Now observe that the subscript a_d no longer represents a single value in the continuum, but the interval $[a-\rho_d/2, a+\rho_d/2]$. The level-crossing behaviour as reflected by $D_{a_d}^x$ should therefore be rather independent of what happens inside this interval. An *approximating alternative view* would consider $[a-\rho_d/2, a+\rho_d/2]$ as the band obtained by blurring the level a with the extremely fast signal $b_\infty(t)$ with $\alpha f_b = \rho_d/2$ (α sufficiently large, e.g. $\alpha = 3$). Then we require that

$$\forall k \geq 1 : D_{ab_\infty}^{x}(1,k\theta_d;f_b = \frac{\rho}{2\alpha}) \overset{(83)}{=} D_a^{xb_\infty}(1,k\theta_d;f_b = \frac{\rho}{2\alpha}) \overset{D}{\simeq} D_a^x(1,k\theta_d) \ , \tag{85}$$

where $\overset{D}{\simeq}$ denotes approximate equality in the sense defined by equation (75). Rigorousness would demand that (85) should be interpreted by discretizing the conditions (65), (66), (67) in the sense that r should be a rational number > 1, but as the rationals are dense in the set of reals, it seems that this step is rather unnecessary from a practical point of view.

A proper selection of (ρ_d, θ_d) could proceed as follows. First select θ_d : it should be sufficiently small so that at least the macroscopic behaviour of the signal will be preserved. All detail on smaller time scales than θ_d will disappear through the discretization. If it is desirable that some microcharacteristic behaviour and the corresponding self-affinity is still observable after discretization, θ_d should be so small that a sufficiently large multiple of θ_d (e.g. $10\theta_d$) still belongs to the microcharacteristic interval. As this interval depends on the specific level under consideration, θ_d will also depend on the detail one wishes to preserve up to a certain level a. For a given θ_d, there is always a minimal level from which on the behaviour under discretization no longer reflects the behaviour of the underlying continuous time signal. Once θ_d is chosen, the f_b-value is selected for which $D_a^{xb\infty}(1, \theta; f_b)$ remains sufficiently close to $D_a^x(1, \theta; f_b)$ for $\theta \geq \theta_d$ in the sense introduced in previous sessions (this itself depends on a prespecified $\delta_{\max}$). Then take $\rho_d = 2\alpha f_b (\alpha = 3 \ldots 4)$.
Another way starts from a given ρ_d (or f_b), while a minimal θ_d (also dependent on $\delta_{\max}$) is derived. Notice that the (ρ_d, θ_d) pair thus found is to be interpreted as giving a maximumvalue for ρ_d and a minimumvalue for θ_d. Increasing ρ_d or decreasing θ_d may start to hide level-crossings of $x(t)$, which are relevant at the time scale θ_d, among the crossings of the blurring signal. On the other hand, decreasing ρ_d will not influence the level-crossing behaviour : only the resolution or separability of the levels will increase. Increasing θ_d would only reduce the microcharacteristic overlap zone I_μ, and this means a loss in relevant or desirable detail.

In the same way, the $D_a^{xb\infty}$-diagrams can be used to derive proper (ρ_d, θ_d) for which the discretized $x_d(t)$ signal still represents the macroscopic behaviour of $x(t)$, when the latter is only known through observation with independent additive noise (noise/signal ratio = f_b). The corresponding (ρ_d, θ_d) should then rather be considered as strict values. This very procedure also gives an answer to the question of assessing the level-crossing activity when disregarding all detail in a band of width $(-\rho_d/2, \rho_d/2)$ around the signal. The mean number of macroscopic level-crossings is given by the mean number of level-crossings of the original signal when sampled at distances $\theta_d(\rho_d)$.

4.4 Blurring with $b_\gamma(t)$ instead of $b_\infty(t)$.

When the extremely fast blurring signal $b_\infty(t)$ is replaced by an "ordinary" fast signal $b_\gamma(t) = b(\gamma t)$, in which γ is the controllable compression-factor (cf. introduction of section 4.2), then zone 3 splits in different new zones. Figure 17 shows some examples. We will discuss the features of the additional zones for the 1st order signal blurred by the 2^{nd}-order signal (fig. 17.b and c).

Zone 6 : $\theta \leq \theta_m$.

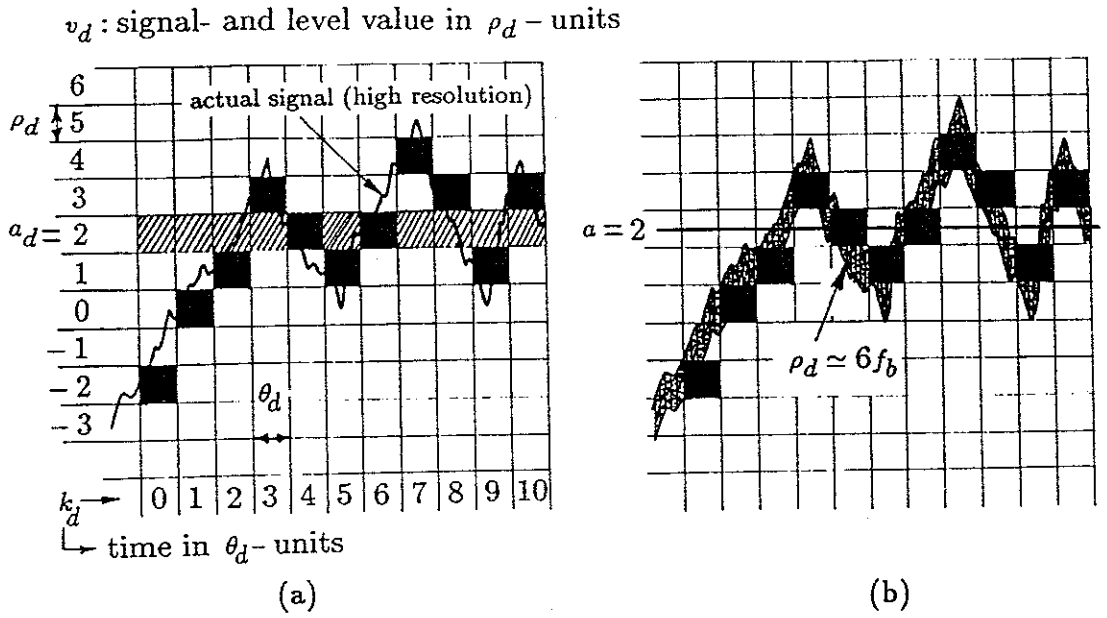


Figure 16: Pixel-based signal representations. Crossings of the original signal $x(t)$ with the discrete value a_d (= hatched band in fig. a) are the same as the crossings of $x(t) \pm \rho_d/2$ with the level a (in fig. b). The latter can be approximated by signal-blurring from which an amplitude-time resolution can be found that produces a $D_a^{xb_\infty}$-behaviour that coincides with the original signal over increasing time scales.

The behaviour in this zone is related to the asymptotic behaviour of the frequency spectrum of $xb_\gamma(t) = (1 - f_b)x(t) + f_b b_\gamma(t)$ for large ω, and is $o[(1 - f_b^2)\omega^{-\beta_x} + f_b^2\omega^{-\beta_{b_\gamma}}] = o[\omega^{-\min(\beta_x, \beta_{b_\gamma})}]$, where β_x and β_{b_γ} are related to x and b_γ respectively). In view of the relationship between β and the limiting value of $D_a(1,\theta)$, we find

$$\lim_{\theta \to 0} D_a^{xb_\gamma}(1,\theta) = \frac{3 - \beta_{xb_\gamma}}{2} = \max[\lim_{\theta \to 0} D_a^x(1,\theta), \lim_{\theta \to 0} D_a^{b_\gamma}(1,\theta)] \ . \qquad (86)$$

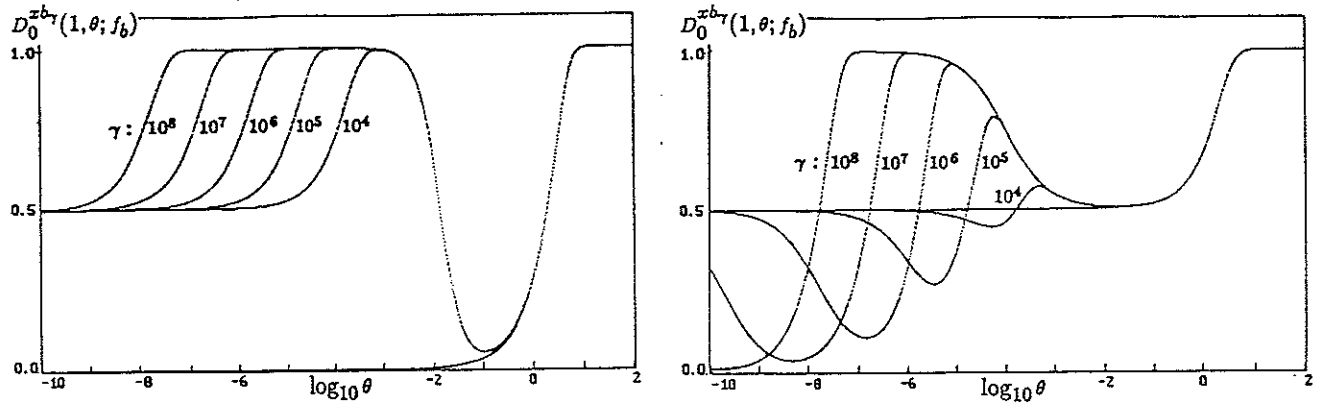
So, in this zone, the $D_a(1,\theta)$-transform of the blurred signal $xb_\gamma(t)$ behaves like the component with the dominating microscopic scale dimension. This is not necessarily the blurring signal. When considering the time domain, this corresponds to the situation where both signals $x(t)$ and $b_\gamma(t)$ exhibit their microcharacteristic behaviour. Invoking formula A2.6, $x(t)$ will dominate if the natural variation of $b_\gamma(t) = b(\gamma t)$ is much smaller than that of $x(t)$, i.e. when

$$\frac{\mu_{b_\gamma}}{\mu_x} f_b^2 \gamma^{2H_{b_\gamma}} \theta^{2(H_{b_\gamma} - H_x)} << 1. \qquad (87)$$

This condition can be satisfied for small θ, only when γ is finite and when $H_{b_\gamma} > H_x$ (or equivalently, when $D_a^{b_\gamma}(1,0) < D_a^x(1,0)$, cf. A2.19). Along the same lines, it can be seen that $b_\gamma(t)$ will dominate when $H_x > H_{b_\gamma}$.

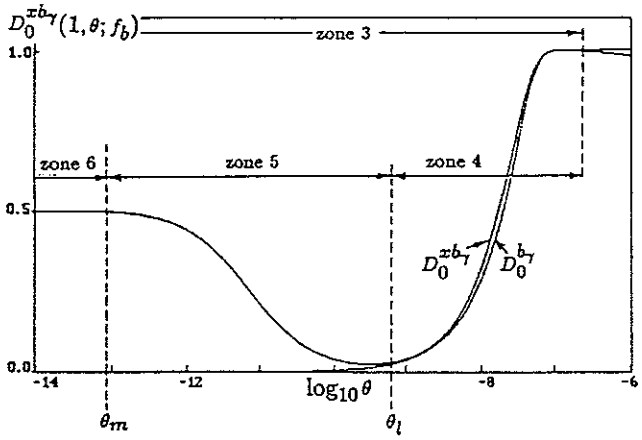
Zone 4 : $\theta_l \leq \theta < \theta_b$.

As can be seen from the enlarged figure 17.c, $D_o^{xb_\gamma}(1,\theta)$ tends to track $D_o^{b_\gamma}(1,\theta)$,



(a)

(b)



(c)

Figure 17: The $D_o(1,\theta)$-transform for a signal $x(t)$ blurred by an "ordinary" fast signal $b_\gamma(t)$.
a : signal $\phi(\tau) = \frac{1}{1-\beta}[\exp(-|\tau| - \beta\exp(-|\tau|/\beta)], \beta = 0.9$ blurred with $\phi_b(\gamma\tau) = \exp(-\gamma|\tau|)$, $(f_b = 0.01)$
b : signal $\phi(\tau) = \exp(-|\tau|)$ blurred by $\phi_b(\gamma\tau) = \frac{1}{1-\beta}[\exp(-\gamma|\tau|) - \beta\exp(-\gamma|\tau|/\beta)]$, $\beta = 0.9, (f_b = 0.01)$
c. Trichotomy of zone 3 for case b with $\beta = 0.9, \gamma = 10^8; f_b = 0.005$.

albeit with a certain shift to the left. The blurring signal clearly dominates at the time-resolution considered. This is a consequence of the fact that for these time scales, local fluctuations of $b_\gamma(t)$ (which are no longer microcharacteristic), are more intense than the microcharacteristic local fluctuations of $x(t)$. The observed left-shift is expected, as $D_o^{xb_\gamma}(1,\theta) = D_{x(t)}^{b_\gamma}(1,\theta)$, where the last symbol considers the crossings of b_γ with the randomly varying level $x(t)$, which is on the average at a certain nonzero distance from the zero-level.

Zone 5 : $\theta_m < \theta < \theta_l$.

This is a transient zone reflecting a smooth transition between zone 6 and 4 as the time resolution changes.

Observe that the width of these zones, and the actual behaviour of $D_a^{xb_\gamma}(1,\theta)$ in them, depend on the nature of the blurring signal and on the blurring factor f_b. Their location depends on the compression-factor γ (the $D_a^{xb_\gamma}$-curves for two different values γ_1 and γ_2 are shifted over a distance $\log \gamma_1/\gamma_2$ as long as the macrobehaviour of $b_{\gamma_i}(t)$ ovelaps the microcharacteristic zone of $x(t)$).

From the examples, we also learn that the occurrence of $D_a^z(1,\theta)$-values close to 1 does not mean that the signal $z(t)$ should be sampling-invariant-independent at the corresponding time scales. It merely indicates that there is an additive component in $z(t)$ that exhibits this feature.

5 Summary

Assessing the level-crossing activity of a stochastic process is a matter of finding the proper time- and amplitude resolution with which the process is observed or represented. The interrelationship of level-crossing rates at different time scales was studied here by means of a scaling-dimensionality transform, first in a general setting, and then for stationary Gaussian processes, which allowed full analytical treatment and provided many examples. This transform emerged from considerations on fractal dimensions. Varying resolutions in amplitude were introduced by means of the concept of controllable signal blurring. A distance concept between different signals based on the scaling dimensionality transform was established. This was helpful in assessing the time- and amplitude scales on which a discretized image of a signal still reflects the proper characteristics of the underlying continuous-time signal. Moreover, the information provided by the transform appeared to be level-dependent at time scales where the signal shows its proper characteristics.

Acknowledgement

The author would like to acknowledge Paul Cauwenberghs for his contributions

(a rather long time ago, while still being a student) in deriving the series representation and the numerical evaluation for $EN_a(\theta)$ as presented in appendix A1.

Appendix 1

A1.1 A series expansion for $EN_a(\theta)$

Let $x_l(t,\theta)$ denote the linearly interpolated version of the process $x(t)$ when sampled with period θ, whereby the initial sampling time is uniformly distributed in $[o,\theta]$ in order to provide overall stationarity of the process (cf. figure 2). The expected number of crossings of the level a in an interval T_o for $x_l(t,\theta)$ is then given by Rice's formula

$$EN_a(T_o,\theta) = T_o \int_{-\infty}^{+\infty} |y| f_{x_l,\dot{x}_l}(a,y)dy = T_o[\int_0^{\infty} y f_{x_l,\dot{x}_l}(a,y)dy + \int_0^{-\infty} y f_{x_l,\dot{x}_l}(a,y)dy] \,, \tag{A1.1}$$

where $f_{x_l,\dot{x}_l}$ is the joint density of $x_l(t)$ and $\dot{x}_l(t)$. It was shown in [10] (formulas 10 to 15) that

$$f_{x_l,\dot{x}_l}(a,y) = \frac{1}{2\pi\sigma_{1\mu}\sigma_{2\mu}\sqrt{1-r_\mu^2}} \int_0^1 \exp(-A)d\mu \tag{A1.2}$$

$$\text{with } A = \frac{1}{2(1-r_\mu^2)}[\frac{a^2\sigma_{2\mu}^2 - 2r_\mu a y \sigma_{1\mu}\sigma_{2\mu} + y^2\sigma_{1\mu}^2}{\sigma_{1\mu}^2\sigma_{2\mu}^2}], \tag{A1.3}$$

$$\text{where } \sigma_{1\mu}^2 \triangleq \sigma_x^2[1 + 2\mu(\mu-1)(1-\phi(\theta))] \tag{A1.4}$$

$$\sigma_{2\mu}^2 \triangleq \frac{2\sigma_x^2}{\theta^2}(1-\phi(\theta)) \tag{A1.5}$$

$$r_\mu\sigma_{1\mu}\sigma_{2\mu} = \frac{\sigma_x^2}{\theta}(1-2\mu)(1-\phi(\theta)), \tag{A1.6}$$

and where $\phi(\theta)$ is the *autocorrelation* function of the signal $x(t)$ at sampling time θ. Where appropriate, $\phi(\theta)$ will be shortened to ϕ in the sequel. Also, the variables $x, x_l, \dot{x}_l, a, y$ will from now on be considered as *normalized with respect to* σ_x (or equivalently, σ_x will be set to 1).

After the proper substitutions of A1.4, A1.5, A1.6 in A1.3, A1.2 and A1.1, we find for the first integral term in (A1.1) :

$$I_1 = \int_0^{\infty} y f_{x_l,\dot{x}_l}(a,y)dy$$

$$= \frac{\theta}{2\pi\sqrt{1-\phi^2}} \int_0^\infty dy \int_0^1 y \exp[-B(y,\mu)] d\mu \ , \qquad \text{(A1.7)}$$

$$\text{with } B(y,\mu) = \frac{a^2(1-\phi) - 2\theta(1-2\mu)(1-\phi)ay + \theta^2(1+2\mu(\mu-1)(1-\phi))y^2}{2(1-\phi^2)} \ .$$

Now introduce the following change of variables

$$\mu = \frac{u-a}{u-v} \quad , y = \frac{u-v}{\theta} \qquad \text{(A1.8)}$$

or equivalently

$$u = a + y\mu\theta \quad v = a + (\mu-1)y\theta. \qquad \text{(A1.9)}$$

This transforms integral (A1.7) into

$$I_1 = \frac{1}{2\pi\sqrt{1-\phi^2}\theta} \int_{-\infty}^a dv \int_a^\infty \exp[-\frac{u^2 - 2uv\phi + v^2}{2(1-\phi^2)}] du \qquad \text{(A1.10)}$$

$$= \frac{1}{\theta} \int_{-\infty}^a dv \int_a^\infty g(u,v,\phi) du, \qquad \text{(A1.11)}$$

where $g(u,v,\phi)$ is the joint normal density of the zero-mean variables u, v with correlation coëfficient ϕ, i.e.,

$$g(u,v,\phi) \triangleq \frac{1}{2\pi\sqrt{1-\phi^2}} \exp[-\frac{u^2 - 2uv\phi + v^2}{2(1-\phi^2)}]. \qquad \text{(A1.12)}$$

Along the same lines, it is found that the second integral term in (A1.1) is equivalent to

$$I_2 = \frac{1}{\theta} \int_a^\infty dv \int_{-\infty}^a g(u,v,\phi) dv \ . \qquad \text{(A1.13)}$$

In the sequel, a number of symbols and properties from Abramowitz & Stegun's Handbook of Mathematical Functions will be used [12]. Formulas from this book will be referred to by their number preceded by the symbol Ab.

Using Ab 26.3.5, 26.3.6, 26.3.7 together with A1.11 and A1.13, produces the following result for A1.1 :

$$EN_a(\theta) = \frac{1}{\theta}[L(-a,a,-\phi) + L(a,-a,-\phi)] = \frac{2}{\theta} L(-a,a,-\phi) \ , \qquad \text{(A1.14)}$$

$$\text{where } L(h,k,\rho) \triangleq \int_h^\infty du \int_k^\infty g(u,v,\rho) dv \ . \qquad \text{(A1.15)}$$

Formula Ab26.3.20 shows that

$$L(-a,a,-\phi) = L(-a,0,\sqrt{\frac{1-\phi}{2}}) + L(a,0,\sqrt{\frac{1-\phi}{2}}) - \frac{1}{2}. \qquad \text{(A1.16)}$$

Invoking Ab26.3.8, 26.2.2, 26.2.3 converts this into

$$L(-a,a,-\phi) = 2L(a,0,\sqrt{\frac{1-\phi}{2}}) - Q(a), \tag{A1.17}$$

$$\text{with } Q(a) \triangleq \frac{1}{\sqrt{2\pi}}\int_{-\infty}^{a} e^{-t^2/2}dt = \frac{1}{2}erfc(a/\sqrt{2}). \tag{A1.18}$$

From A1.14 and A1.16 we obtain :

$$EN_a(\theta) = \frac{4}{\theta}[L(a,0,\sqrt{\frac{1-\phi(\theta)}{2}}) - \frac{1}{2}Q(a)]. \tag{A1.19}$$

Ab26.3.29 gives the following series expansion for the L-term

$$L(a,0,\sqrt{\frac{1-\phi(\theta)}{2}}) = Q(a)Q(0) + \sum_{n=0}^{\infty}\frac{Z^{(n)}(a)Z^{(n)}(0)}{(n+1)!}(\frac{1-\phi(\theta)}{2})^{\frac{n+1}{2}}, \tag{A1.20}$$

where $Z^{(n)}(x)$ is the n-th derivative of

$$Z(x) \triangleq \frac{1}{\sqrt{2\pi}}\exp(-x^2/2) \ . \tag{A1.21}$$

Using Ab 26.2.28, 26.2.32 and the fact that $Q(0) = 1/2$ in A1.20, reshapes A1.19 into

$$EN_a(\theta) = \frac{2}{\pi\theta}\exp(-a^2/2)\sqrt{\frac{1-\phi}{2}}\sum_{n=0}^{\infty}\frac{(-1)^n H_{2n}(a/\sqrt{2})}{2^{2n}n!(2n+1)}(\frac{1-\phi}{2})^n, \tag{A1.22}$$

with $H_n(x)$ being the Hermite-polynomial of degree n. Relating the Hermite-polynomial to the generalized Laguerre polynomial of degree n through Ab 22.5.40 ultimately produces

$$EN_a(\theta) = \frac{2}{\pi\theta}\exp(-\frac{a^2}{2})\sqrt{\frac{1-\phi(\theta)}{2}}\sum_{n=0}^{\infty}\frac{L_n^{(-1/2)}(a^2/2)}{2n+1}\cdot(\frac{1-\phi(\theta)}{2})^n. \tag{A1.23}$$

A1.2 · An alternative expression for $EN_a(\theta)$.

$EN_a(\theta)$ and $EN_o(\theta)$ are related in the following way :

$$EN_a(\theta) = EN_o(\theta) - \frac{2}{\pi\theta}\int_0^a dx\int_o^x \sqrt{\frac{1-\phi(\theta)}{1+\phi(\theta)}}\exp(-\frac{x^2+y^2}{2})dy. \tag{A1.24}$$

<u>Proof</u> : Ab 26.3.7 and Ab 26.3.8 show that

$$L(-a,0,\sqrt{\frac{1-\phi}{2}}) = \frac{1}{2} - L(a,0,-\sqrt{\frac{1-\phi}{2}}) \tag{A1.25}$$

$$L(a,0,\sqrt{\frac{1-\phi}{2}}) = L(0,a,\sqrt{\frac{1-\phi}{2}}) = Q(a) - L(a,0,-\sqrt{\frac{1-\phi}{2}}) \ . \quad \text{(A1.26)}$$

Using (A1.25), (A1.26) in (A1.16) gives

$$\begin{aligned} L(-a,a,-\phi) \ &= \ -2L(a,0,-\sqrt{\frac{1-\phi}{2}}) + Q(a) \\ &\quad - 2[\frac{1}{4} + L(a,0,-\sqrt{\frac{1-\phi}{2}}) - L(0,0,-\sqrt{\frac{1-\phi}{2}}) - \frac{1}{2}Q(a)] \\ &\quad + \frac{1}{2} - 2L(0,0,-\sqrt{\frac{1-\phi}{2}}) \ . \end{aligned} \quad \text{(A1.27)}$$

Invoking Ab 26.3.23 and 26.3.19 to reinterprete A1.27 produces the following equivalent expression for A1.14

$$EN_a(\theta) = \frac{2}{\pi\theta}\arcsin\sqrt{\frac{1-\phi}{2}} - \frac{2}{\pi\theta}\int_0^a dx \int_0^x \sqrt{\frac{1-\phi}{1+\phi}} \exp(-\frac{x^2+y^2}{2})dy. \quad \text{(A1.28)}$$

It follows that the arcsin-term equals $EN_o(\theta)$ $(= (\pi\theta)^{-1}\arccos\phi)$, hence this expression is equivalent to (A1.24).

A1.3 Differentiating $EN_a(\theta)$.

a. Derivation of $\frac{\partial EN_a(\theta)}{\partial\theta}$

Observe from A1.23 that $EN_a(\theta) = f(\theta,\phi(\theta))$. So,

$$\frac{\partial EN_a(\theta)}{\partial\theta} = -\frac{1}{\theta}EN_a(\theta) + \frac{\partial EN_a(\theta)}{\partial\phi}\cdot\frac{\partial\phi(\theta)}{\partial\theta}, \quad \text{(A1.29)}$$

with

$$\frac{\partial EN_a(\theta}{\partial\phi} = -\frac{1}{2\pi\theta}\exp(-\frac{a_n^2}{2})(\frac{1-\phi}{2})^{-1/2}\sum_{n=0}^{\infty} L_n^{(-1/2)}(a_n^2/2)(\frac{1-\phi}{2})^n. \quad \text{(A1.30)}$$

From the generating function of the Laguerre-polynomials, we find [Ab 22.9.15] that the last summation is equal to

$$(\frac{1+\phi}{2})^{-1/2}\exp(-\frac{a_n^2}{2}\cdot\frac{1-\phi}{1+\phi}) \ . \quad \text{(A1.31)}$$

Backtracking to (A1.29) results in

$$\frac{\partial EN_a(\theta)}{\partial\theta} = -\frac{1}{\theta}EN_a(\theta) - \frac{1}{\pi\theta\sqrt{1-\phi^2}}\exp(-\frac{a_n^2}{1+\phi})\cdot\frac{\partial\phi(\theta)}{\partial\theta} \ . \quad \text{(A1.32)}$$

b. Derivation of $\frac{\partial EN_a(\theta)}{\partial a}$.

It readily follows from (A1.24) that

$$\frac{\partial EN_a(\theta)}{\partial a} = -\frac{1}{\theta}\sqrt{\frac{2}{\pi}}\exp(-\frac{a^2}{2})erf(\frac{a}{2}\sqrt{\frac{1-\phi}{1+\phi}}) \quad . \tag{A1.33}$$

From the definition of $D_a(r,\theta)$ (equations 12, 13), we find

$$\frac{\partial D_a(r,\theta)}{\partial a} = \frac{1}{\theta EN_a(\theta)}[\frac{\partial EN_a(\theta)}{\partial a} - r^{D_a(r,\theta)-1}\frac{\partial EN_a(r\theta)}{\partial a}]/\log r \ . \tag{A1.34}$$

With (A1.33), this transforms into

$$\frac{\partial D_a(r,\theta)}{\partial a} = \frac{-erf(\frac{a}{\sqrt{2}}\sqrt{\frac{1-\phi(\theta)}{1+\phi(\theta)}}) + r^{D_a(r,\theta)-1}erf(\frac{a}{\sqrt{2}}\sqrt{\frac{1-\phi(r\theta)}{1+\phi(r\theta)}})}{\log r} \cdot \sqrt{\frac{2}{\pi}}\frac{\exp(-\frac{a^2}{2})}{\theta EN_a(\theta)} \tag{A1.35}$$

From this, it can be derived that the following properties hold :

a. $\forall r,\theta:\ \frac{\partial D_a(r,\theta)}{\partial a}|_{a=0} = 0$ (A1.36)

b. $\forall a,r:\ \lim_{\theta\to 0}\frac{\partial D_a(r,\theta)}{\partial a} = 0$ (when $\phi(\theta)$ is continuous at $\theta = 0$) (A1.37)

c. $\forall a,r:\ \lim_{\theta\to\infty}\frac{\partial D_a(r,\theta)}{\partial a} = 0$ (when $\lim_{\theta\to\infty}\phi(\theta) = 0$) (A1.38)

Calculating the 2nd derivative of $D_a(r,\theta)$ with respect to the level a, gives the surprisingly simple result at $a = 0$:

$$\frac{\partial^2 D_a(r,\theta)}{\partial a^2}|_{a=0} = \frac{\frac{\sqrt{\frac{1-\phi(r\mu)}{1+\phi(r\mu)}}}{\arccos\phi(r\mu)} - \frac{\sqrt{\frac{1-\phi(\mu)}{1+\phi(\mu)}}}{\arccos\phi(\mu)}}{\log r} \quad . \tag{A1.39}$$

A1.4 Numerical evaluation and accuracy of $EN_a(\theta)$.

Introduce $q(\theta) \triangleq [1-\phi(\theta)]/2$ and recall formula A1.23

$$EN_a(\theta) = \frac{2}{\pi\theta}\exp(-\frac{a^2}{2})\sqrt{q(\theta)}\sum_{n=0}^{\infty}\frac{L_n^{(-1/2)}(a^2/2)}{2n+1}q^n(\theta). \tag{A1.40}$$

Define

$$V_n(\alpha,q) = L_n^{(-1/2)}(\alpha)q^n, \tag{A1.41}$$

then

$$EN_a(\theta) = \frac{2}{\pi\theta}\exp(-\frac{a^2}{2})\sqrt{q(\theta)}\sum_{n=0}^{\infty}\frac{V_n(a^2/2,q(\theta))}{2n+1}. \tag{A1.42}$$

Numerical evaluation of $EN_a(\theta)$ will be done by performing the summation up to the $(m+1)^{th}$ term, with m sufficiently large in a way to be derived further. $L_{n+1}^{(-1/2)}(\alpha)$ satisfies the recurrence relation (Ab.22.7.12)

$$(n+1)L_{n+1}^{(-1/2)}(\alpha) + (\alpha - 2n - \frac{1}{2})L_n^{(-1/2)}(\alpha) + (n - \frac{1}{2})L_{n-1}^{(-1/2)}(\alpha) = 0 \quad \text{(A1.43)}$$

with initial values $L_0^{(-1/2)}(\alpha) = 1$ and $L_1^{(-1/2)}(\alpha) = \frac{1}{2} - \alpha$.
Multiplying (A1.43) by q^2 produces the following recursion in $V(\alpha, q)$ which can directly be used in (A1.42) :

$$(n+1)V_{n+1}(\alpha,q) + (\alpha - 2n - \frac{1}{2})qV_n(\alpha,q) + (n - \frac{1}{2})q^2V_{n-1}(\alpha,q) = 0 \quad \text{(A1.44)}$$

with corresponding initial conditions

$$V_0(\alpha,q) = 1 \text{ and } V_1(\alpha,q) = (\frac{1}{2} - \alpha)q.$$

We will now derive an upper bound for the remainder in the summation in (A1.40) when it is truncated after the $(m+1)^{th}$ term :

$$R_m(a_n, q(\theta)) \triangleq \sum_{n=m+1}^{\infty} \frac{L_n^{(-1/2)}(a_n^2/2)}{2n+1} q^n(\theta) \ . \qquad \text{(A1.45)}$$

Ab.22.5.38 and 22.14.17 show that

$$|L_n^{(-1/2)}(a_n^2/2)| = \frac{|H_{2n}(a_n/\sqrt{2})|}{n!2^{2n}} < \frac{\exp(a_n^2/4)k2^n\sqrt{(2n)!}}{n!2^{2n}} \quad , \qquad \text{(A1.46)}$$

with $k \simeq 1.086435$.
It follows that

$$|R_m(a_n,q)| < \sum_{n=m+1}^{\infty} \frac{|L_n^{-1/2}(a_n^2/2)|}{2n+1} q^n < k\exp(a_n^2/4) \sum_{n=m+1}^{\infty} \frac{\sqrt{(2n)!}}{n!2^n(2n+1)} q^n \ . \qquad \text{(A1.47)}$$

Using Sterling's formula for the factorials (Ab 6.1.38) transforms the right-hand member of this inequality into

$$\frac{k\exp(a_n^2/4)}{\pi^{1/4}} \sum_{n=m+1}^{\infty} \frac{(q/e)^n}{n^{1/4}(2n+1)} \exp(\frac{\theta_1 - 2\theta_2}{24n}) \quad , \qquad \text{(A1.48)}$$

with $0 < \theta_1, \theta_2 < 1$. These conditions on θ_1, θ_2 imply that $-2 < \theta_1 - 2\theta_2 < 1$. Hence, for all $n \geq m+1$:

$$\exp(\frac{\theta_1 - 2\theta_2}{24n}) < \exp(\frac{1}{24(m+1)}), \qquad \text{(A1.49)}$$

and it follows that

$$\text{expression (A1.48)} \quad < \frac{k \exp(a_n^2/4) \exp(\frac{1}{24(m+1)})}{\pi^{1/4} m^{1/4} (2m+3)} \sum_{n=m+1}^{\infty} (q/e)^n \; . \qquad \text{(A1.50)}$$

As $q \triangleq \frac{1-\phi}{2} \leq 1$, the last summation converges to $(q/e)^{m+1}(1-q/e)^{-1}$. This has its maximum for $q = 1$ and equals $1/e^m(e-1)$. Tracing back to A1.47 then ultimately gives the uniform upper bound

$$|R_m(a_n, q)| < \frac{k \exp(a_n^2/4) \exp(\frac{1}{24(m+1)})}{\pi^{1/4} m^{1/4} (2m+3)(e-1)} e^{-m} \; . \qquad \text{(A1.51)}$$

Or, as a less tight upper bound

$$|R_m(a_n, q)| < \frac{k \exp(a_n^2/4) \exp(1/24)}{\pi^{1/4}(e-1)} e^{-m} \; . \qquad \text{(A1.52)}$$

If $\varepsilon_{\max} > 0$ is the maximal error to be tolerated in the evaluation of the sum in A1.40 by truncating the series, a lower bound on m that guarantees this can be found from (A1.51) or (A1.52) by requiring that the right hand expressions be smaller than $\varepsilon_{\max}$.
(A1.52) readily provides an explicit condition :

$$m > \log \frac{k \exp(a_n^2/4) \exp(1/24)}{\pi^{1/4}(e-1)\varepsilon_{\max}} = \frac{a_n^2}{4} - \log \varepsilon_{\max} - 0.70293 \; . \qquad \text{(A1.53)}$$

If $\varepsilon_{\max}$ represents a required accuracy up to the Nth place after the decimal point, then $\varepsilon_{\max} = 10^{-(N+1)}$ and (A1.53) becomes

$$m > \frac{a_n^2}{4} + N \log 10 + 1.6 \; . \qquad \text{(A1.54)}$$

Appendix 2

1. The behaviour of the correlation function $\phi(\tau)$ for small τ and for the different categories I to IV, as presented in section 3.2 is given by the general expression

$$\phi(\tau) = 1 - \mu\tau^{2H} + \gamma\tau^2 + o(\tau^{2H}) \; . \qquad \text{(A2.1)}$$

In particular, for the Bessel-type correlation function (52) in the categories I-II-III, it can be derived that

$$\text{for } \frac{1}{2} < \nu < \frac{3}{2} : \phi_\nu(\tau) = 1 - \frac{\Gamma(\frac{3}{2}-\nu)}{2^{2\nu-1}\Gamma(\nu+\frac{1}{2})}\tau^{2(\nu-\frac{1}{2})} + \frac{\Gamma(\frac{3}{2}-\nu)}{4\Gamma(\frac{5}{2}-\nu)}\tau^2 + o(\tau^2) \; . \qquad \text{(A2.2)}$$

This was obtained by using the Bessel-function properties (9.6.2), (9.6.10) and (6.1.17) in Abramowitz [12] while calculating the product $\tau K_1(\tau)$, and retaining the lowest-order terms in the series expansion.
For $\nu = \frac{3}{2}$, the following special result emerges (using 9.6.11 and 9.6.10 in [12])

$$\begin{aligned} \phi_{\frac{3}{2}}(\tau) &= 1 + I_1(\tau)\log\tfrac{\tau}{2} + O(\tau^2) \\ &\simeq 1 + \tfrac{\tau}{2}\log\tfrac{\tau}{2} + O(\tau^2) \quad , \end{aligned} \tag{A2.3}$$

where in general, $\tau^\alpha \log\tau = O(\tau^\beta)$ for $o < \beta < \alpha$.
For the class-II nondifferentiable signals, we have

$$\phi(\tau) = 1 + \dot{\phi}(o^+)\tau + \frac{1}{2}\ddot{\phi}(o^+)\tau^2 \tag{A2.4}$$

and, for the class-IV of common differentiable signals

$$\phi(\tau) = 1 + \frac{1}{2}\ddot{\phi}(o)\tau^2 + \frac{1}{6}\dddot{\phi}(o^+)\tau^3 . \tag{A2.5}$$

2. The expected value of the squared increment over small τ is then given by

$$E[\Delta^2 x(\tau)] \triangleq E[x(t+\tau) - x(t)]^2 = 2\sigma_x^2[1 - \phi(\tau)] \simeq 2\mu\tau^{2H}\sigma_x^2 \ . \tag{A2.6}$$

3. Derivation of $D_o(\tau, \theta)$ for small θ.
Referring to formula (47), this requires the calculation of $\log\arccos\phi(\tau)$.
For the Bessel-type correlation functions with $0.5 < \nu = H + 0.5 < 1.5$, the use of (A2.1) leads to

$$\arccos\phi(\tau) = \arcsin\sqrt{1 - \phi^2(\tau)} = \arcsin\sqrt{2\mu\tau^{2H} - 2\gamma\tau^2 - \mu^2\tau^{4H} + O(\tau^{2(H+1)})}. \tag{A2.7}$$

Invoking the series expansion of the arcsin-function, and retaining the lowest order terms transforms this in

$$\sqrt{2\mu\tau^{2H}}\sqrt{1 - \frac{\gamma}{\mu}\tau^{2(1-H)} - \frac{\mu}{2}\tau^{2H} + O(\tau^2)}\cdot[1 + \frac{1}{6}(2\mu\tau^{2H} - 2\gamma\tau^2 - \mu^2\tau^{4H} + O(\tau^{2(H+1)}) + \ldots]. \tag{A2.8}$$

The second square-root factor can be approximated by the lowest order terms of its power-series expansion as

$$1 - \frac{\gamma}{2\mu}\tau^{2(1-H)} - \frac{\mu}{4}\tau^{2H} + \ldots$$

Using this in (A2.8), and working out the products results in the following approximations, the lowest order terms of which depend on the value of H.

$$\arccos\phi(\tau) \simeq \sqrt{2\mu\tau^{2H}}[1+\frac{\mu}{12}\tau^{2H}] \text{ for } H<0.5 \quad \text{(A2.9)}$$

$$\arccos\phi(\tau) \simeq \sqrt{2\mu\tau^{2H}}[1-\frac{\gamma}{2\mu}\tau^{2(1-H)}] \text{ for } H>0.5 \quad \text{(A2.10)}$$

$$\arccos\phi(\tau) \simeq \sqrt{2\mu\tau^{2H}}[1+(\frac{\mu}{12}-\frac{\gamma}{2\mu})\tau] \text{ for } H=0.5 \quad \text{(A2.11)}$$

With $\delta_H(\tau)$ the τ-dependent term inside the square brackets, this gives

$$\begin{aligned}\log\arccos\phi(\tau) &\simeq \tfrac{1}{2}\log 2\mu + H\log\tau + \log(1+\delta_H(\tau)) \\ &\simeq \tfrac{1}{2}\log 2\mu + H\log\tau + \delta_H \ .\end{aligned} \quad \text{(A2.12)}$$

Inserting this last result in (47), we get the following approximation for sufficiently small θ :

$$D_o(r,\theta) \simeq (1-H)+\frac{\delta_H(\theta)-\delta_H(r\theta)}{\log r} \quad \text{(A2.13)}$$

$$\simeq (1-H)+\frac{\mu}{12}\frac{\theta^{2H}[1-r^{2H}]}{\log r} \text{ for } H<0.5 \quad \text{(A2.14)}$$

$$\simeq (1-H)-\frac{\gamma}{2\mu}\frac{\theta^{2(1-H)}[1-r^{2(1-H)}]}{\log r} \text{ for } H>0.5 \quad \text{(A2.15)}$$

$$\simeq (1-H)+(\frac{\mu}{12}-\frac{\gamma}{2\mu})\frac{\theta[1-r]}{\log r} \text{ for } H=0.5 \ . \quad \text{(A2.16)}$$

$D_o(1,\theta)$ is found by taking the appropriate limit which makes the r-dependent factor equal to 1. For the signals in class II with a correlation function satisfying (A2.4), $H=0.5$, and (A2.16) transforms into

$$D_o(r,\theta) \simeq \frac{1}{2}-[\frac{\dot\phi(o^+)}{12}-\frac{\ddot\phi(o^+)}{4\dot\phi(o^+)}]\cdot\frac{1-r}{\log r}\cdot\theta \quad \text{(A2.17)}$$

A similar calculation can be performed on the mean square differentiable signals with correlation type (A2.5), for which $H=1$. This produces

$$D_o(r,\theta) \simeq \frac{1}{6}\frac{\dddot\phi(o^+)}{\ddot\phi(o^+)}\frac{1-r}{\log r}\theta \ . \quad \text{(A2.18)}$$

Observe that all these expressions have the same form

$$D_o(r,\theta) \simeq (1-H)+\alpha\frac{1-r^\chi}{\log r}\theta^\chi \quad \text{(A2.19)}$$

$(\chi=\min(2H,2(1-H))$ for $H<1, \chi=1$ for $H=1)$.

It follows that $\lim_{\theta\to 0} D_o(r,\theta) = 1 - H$, the fractal dimension of the level-crossing set of the fractional Brownian motions to which the signals tend microscopically (classes I, II, III). For class-IV signals, $D_o(r,0) = 0$ and equals the topological dimension of a point set. Therefore, these signals will usually not be considered as fractals.

Appendix 3

Formulas (A2.2), (A2.19), (A2.9,10,11) and (63) lead to the following expressions for the upper bound θ_c of the microcharacteristic interval as given by (64). These expressions are valid as long as the resulting $\theta_c << 1$.

1. For the signals with the Bessel-type correlation functions (eqn. 52), one finds :

$$\text{for} \quad H = \nu - 0.5 = 0.5 : \theta_c \simeq 6\delta_{\max} \tag{A3.1}$$

$$H = \nu - 0.5 < 0.5 : \theta_c \simeq 2[\frac{12\Gamma(1+H)}{\Gamma(1-H)}\delta_{\max}]^{1/2H} \tag{A3.2}$$

$$\text{with } \lim_{H\to 0.5-} \theta_c \simeq 12\delta_{\max}$$

$$0.5 < H = \nu - 0.5 < 1 : \theta_c \simeq [\frac{8\Gamma(2-H)}{2^{2H}\Gamma(1+H)}\delta_{\max}]^{1/2(1-H)} \tag{A3.3}$$

$$\text{with } \lim_{H\to 0.5+} \theta_c \simeq 4\delta_{\max} \ , \ \lim_{H\to 1-} \theta_c \simeq 0$$

2. For the common type-II non-differentiable signals, we obtain

$$\theta_c \simeq \frac{\delta_{\max}}{|\frac{\dot{\phi}(o^+)}{12} - \frac{\ddot{\phi}(o^+)}{4\dot{\phi}(o^+)}|} \tag{A3.4}$$

The results for a few common signals are given in the following table :

Correlation function	θ_c(eqn. 64)
$e^{-\lvert\tau\rvert}$	$6\delta_{\max}$
$\max(0, 1 - \lvert\tau\rvert)$	$12\delta_{\max}$
$e^{-\lvert\tau\rvert}\cos\omega_o\tau$	$12\delta_{\max}/\lvert 2 - 3\omega_o^2\rvert$
$\frac{1}{\beta-1}(\beta e^{-\lvert\tau\rvert} - e^{-\lvert\tau\rvert/\beta})$	$\frac{12\beta(1+\beta)}{3\beta^4+3\beta^3+2\beta^2-2\beta-1}\delta_{\max}$

3. For the common type-IV differentiable signals, the following result is found :

$$\theta_c \simeq 6|\frac{\ddot{\phi}(o^+)}{\dddot{\phi}(o^+)}|\delta_{\max} \ . \qquad \text{(A3.5)}$$

For the signal with correlation function $\frac{1}{1-\beta}(e^{-|\tau|} - \beta e^{-|\tau|/\beta})$, this gives

$$\theta_c \simeq \frac{6\beta}{1+\beta}\delta_{\max}.$$

References

[1] I.F. Blake and W.C. Lindsay : "Level-crossing problems for random processes", *IEEE Trans. Inform. Theory*, vol. IT-19, no. 3, pp. 295-315, 1973.

[2] J. Abrahams, "A survey of recent progress on level-crossing problems for random processes", in *Communications and Networks - A Survey of Recent Advances*, New York : Springer Verlag, 1986.

[3] A.J. Rainal, "Origin of Rice's formula", *IEEE Trans. Inform. Theory*, vol. IT-34, no. 6, pp. 1383-1387, 1988.

[4] S.O. Rice, "Mathematical analysis of random noise", *Bell Syst. Tech. J.*, vol. 23, pp. 282-332, July 1944; vol. 24, pp. 46-156, Jan. 1945.

[5] M. Kac, "On the average number of real roots of a random algebraic equation", *Bull. Amer. Math. Soc.*, vol. 49, pp. 314-320, 1943.

[6] H. Cramér and M.R. Leadbetter, *Stationary and Related Stochastic Processes*, New York : Wiley, 1967.

[7] B.B. Mandelbrot and J.W. Van Ness, "Fractional Brownian motions, fractional noises and applications", *SIAM Review*, vol. 10, no. 4, pp. 422-437, 1968.

[8] B.B. Mandelbrot, "*The Fractal Geometry of Nature*", New York, W.H. Freeman; 1983 ed.

[9] R.F. Voss, "Fractals in nature : from characterization to simulation", in *The Science of Fractal Images*, New-York : Springer Verlag, 1988.

[10] A.M. Barbé, "A measure for the mean level-crossing activity of stationary normal processes", *IEEE Trans. Inform. Theory*, Vol. IT-22, no. 1, pp. 96-102, 1976.

[11] M.F. Barnsley, "*Fractals Everywhere*", San Diego : Academic Press, 1988.

[12] M. Abramowitz and I.A. Stegun, "*Handbook of Mathematical Functions*", New York : Dover Publications, 9th printing (1970).

[13] H.G. Schuster, "*Deterministic Chaos, An Introduction*", Weinheim : Physik-Verlag, 1984.